Performance of home of flood resiliency and flood retrofit measures

Poirier, Louis; Stolle, Jacob; Knox, Paul

Publisher’s version / Version de l'éditeur:
https://doi.org/10.4224/40003478
Technical Report (National Research Council of Canada. Ocean, Coastal and River Engineering Research Centre); no. NRC-OCRE-2025-TRQ-005, 2025-03-28

Performance of Home of Flood Resiliency and Flood Retrofit Measures

Report No.: NRC-OCRE-2025-TRQ-005

Prepared for: Élène Levasseur
Directrice de recherche et éducation
Architecture Sans Frontières Québec
elevasseur@asfq-quebec.org

Revision 1.4
Date: 2025-03-28

Authors: Louis Poirier, Jacob Stolle, and Paul Knox

Ocean, Coastal, and River Engineering
Research Centre

National Research Council Canada
Conseil national de recherches Canada

Revision History

Document Version	Name	Affiliation	Date of Changes	Comments
1.0	Jacob Stolle	INRS	26 Jan. 2025	Draft Report
1.1	Louis Poirier	NRC-OCRE	26 Feb. 2025	Content Additions
1.2	Jacob Stolle	INRS	6 Mar. 2025	Corrections
1.3	Paul Knox	NRC-OCRE	18 Mar 2025	NRC Internal Review
1.4	Louis Poirier	NRC-OCRE	26 Mar. 2025	Response to comments

Executive Summary

This report outlines a study funded by Architecture Sans Frontières Québec (ASFQ) and Canada Mortgage and Housing Corporation (CMHC) as part of the “Building for the Future” initiative. Flooding remains the costliest natural hazard worldwide, with damage exceeding US$320 billion from 2018 to 2023. Increasing instances of flooding, fueled by climate change, aging infrastructure and extreme weather conditions, present serious risks, particularly in Canada, where 80% of cities are located in flood-prone areas. With a significant proportion of Canada's real estate stock located in flood-prone areas, cost-effective solutions are essential to protect these properties. This project aims to:

- Evaluate the effectiveness of Canadian building standards against the effect of floods.
- Evaluate various temporary residential flood barriers under different conditions.
- Develop experimental protocols in line with existing international standards.

Two phases of testing were carried out at the National Research Council of Canada (NRC):

- Phase 1: focused on assessing performance (leakage rates) through standard Canadian residential construction.
- Phase 2: evaluated the performance of various temporary opening flood barriers in two experimental setups (Figure 1)

Figure 1. Phase 2 wave tests of four opening flood barriers in the National Research Council's (NRC) Multidirectional Wave Basin (MWB). From left to right: plywood, Flow Stop full sized cushion (Mono), sandbags and Flow Stop regular cushion (Bi).

Overview

Phase 1: Standard residential construction (NBC, 2020)

1. Leakage behavior:
    a. Leakage rates were highest at between the sill plate and the foundation, followed by leakage between the door and its frame.
    b. Increasing water depth correlated with higher leakage rates, although wood expansion reduced leakage over time.

Phase 2 Opening barriers

1. Barrier performance (Figure 2) :
    a. Proprietary barriers outperformed traditional measures (sandbags, plywood).
    b. Leakage rates for most barriers exceeded the levels suggested by ANSI 2510, particularly at greater water depths.
    c. Some barriers failed under wave action and debris impact due to displacement or detachment from the opening or component failure.
2. Influence of water level:
    a. Performance decreased as the depth of water above the opening sill increased.
    b. The main source of leakage was between the base of the barrier and its frame. Overflow, or wave overtopping only occurred for barriers that did not completely fill the opening and at the highest wave height.
3. Comparison with ANSI standards:
    a. Testing revealed discrepancies between actual performance and ANSI-certified results, highlighting the need for specific and localized testing, a need to investigate repeatability effects, and clearer testing guidelines.

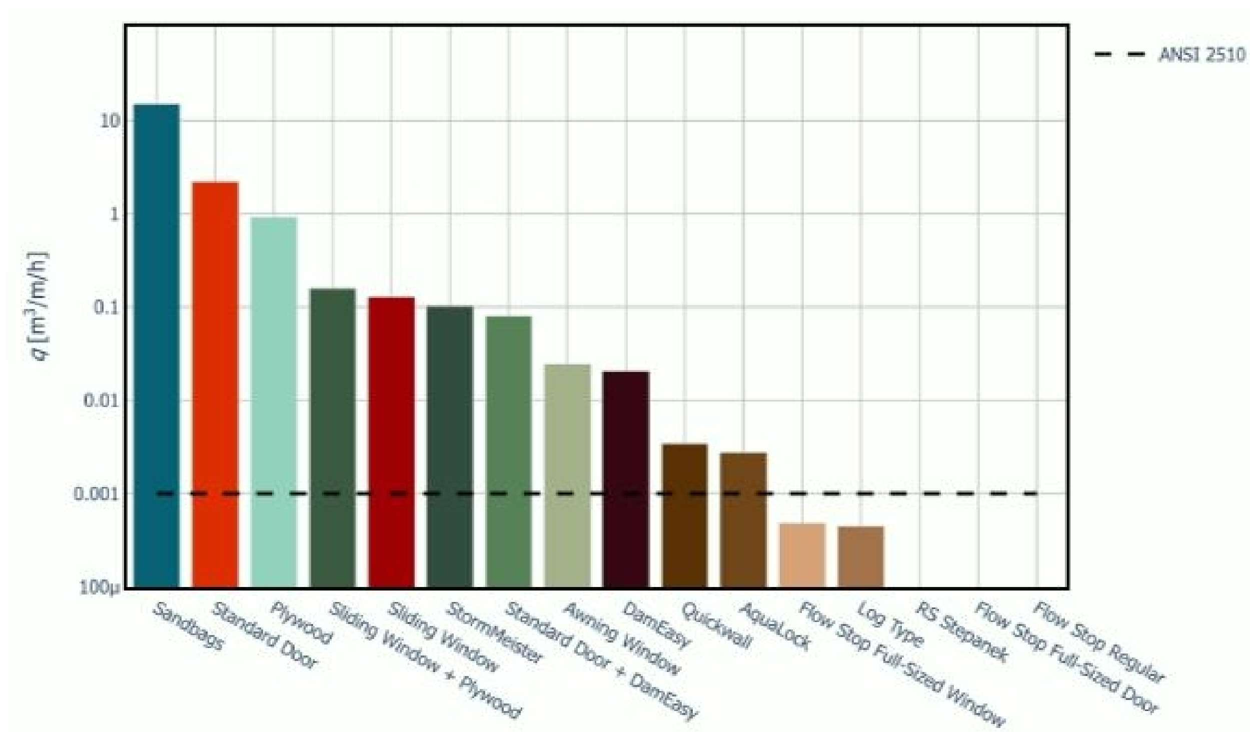

Figure 2. Summary of opening barrier performance in Phase 2 experiments at water level (0.585 m). Leakage rates are presented as volume flows per unit meter, and the ANSI 2510 threshold for opening barriers is represented by a dashed black line.

Key findings and future recommendations

1. Improve test standards:
    a. Develop Canadian-specific test protocols to ensure barrier suitability and reliability under regional conditions.
    b. Establish clearer guidelines for barrier installation to minimize user error.
    c. The results of this study will be forwarded to the committee working on the development of a testing standard for perimeter barriers, with the goal of including opening barriers in a future edition (CSA, 2025).
2. Improved testing:
    a. Conduct repeated testing on various Canadian building envelopes to account for construction variability and develop an understanding of acceptable margins of error.
    b. Include interdisciplinary research on moisture damage and structural performance and integrity.
3. Public confidence:
    a. Increase transparency of experimental methods and results to build confidence in flood mitigation solutions.
    b. Promote education on proper installation and maintenance of flood barriers.
4. Training of highly qualified personnel
    a. The project contributed to the training and further education of four highly qualified personnel at INRS: two undergraduate research trainees and two PhD students.

This study highlights the critical need for adaptable, standardized flood protection measures tailored to Canadian contexts. While many of the proprietary flood barriers tested showed promise, performance inconsistencies under real-world conditions underscore the need for rigorous, standardized testing. The knowledge gained here has laid the foundation for future research, policy development and public adoption of effective flood mitigation strategies.

Results

This study is one of the first in the world to comprehensively compare temporary opening barriers (traditional and proprietary) in a three-dimensional flood environment with waves and debris impacts. The knowledge gained from this study will assist the general public in barrier selection and serve as a benchmark for the development of improved testing standards in Canada.

The results of this study will be forwarded to the CSA working group developing the standard for temporary flood barriers. The project also contributed to the training of four highly qualified people at INRS: two undergraduate research trainees and two doctoral students.

Table of Contents

List of Figures

List of Tables

1. Introduction

1.1. Background

Flooding is the costliest natural hazard in the world. From 2018 – 2023, losses due to flooding amounted to over $320 billion USD (Ellenrieder & Rauch, 2024). The occurrence of flood events is expected to rise over the next century due to the impacts of climate change including increased precipitation, aging infrastructure, and increased storms (Intergovernmental Panel on Climate Change (IPCC), 2023). Within Canada, the vast majority of Canadian cities (~80%) are located within a flood zone (Environment and Climate Change Canada, 2024). In Quebec, flooding can arise from a variety of sources and environments (Déry et al., 2023), including:

- Spring Freshet (example: Montreal, 2019)
  - Flooding associated with the melting of snow and episodes of precipitation on melting snow occurring in the spring.
- Open Water (Outaouais, 2011)
  - Flooding associated with high river discharges from intense or long duration precipitation occurring in the summer or fall.
- Winter (Saint-Raymond de Portneuf, 2012)
  - Flooding caused by ice jam formation during freeze-thaw cycles or ice breakup occurring in winter and early spring.
- Coastal (Îles-de-la-Madelaine, 2022)
  - Flooding associated with large coastal storms where high winds and low pressure can induce storm surge which can occur any time of year, though normally in late fall/early winter.
- Urban (Montreal, 2023)
  - Flooding associated with the overflow of storm systems due to intense (often short duration) precipitation.
- Aging Infrastructure (Montreal, 2024)
  - Flooding associated with aging or insufficient infrastructure that fails resulting in the release of a large quantity of water.

Considering the widespread occurrence and variety of flood events across Quebec, major infrastructure investment can only do so much to combat the impacts of climate change. Therefore, for the approximately 77 000 houses that are within the flood zones of Quebec, infrastructure across large scales may not always be possible. Considering that some of these houses remain important to the cultural heritage of Quebec (Déom, 2024) and critical to the available housing stock within the province (Public Security Canada, 2022), options are needed to protect and maintain these properties.

The ASFQ proposed a range of options for living with water, including adaptation measures to avoid, resist, or accommodate flood events (Levasseur, 2021). This project will specifically focus on the resist component of living with water, focusing on low-cost solutions for retrofitting houses to respond to flood events. Many options exist including flood-resilient cladding and elevating the house or foundation, however, to address the low-cost option, this project focuses specifically on temporary removable flood barriers at a residential scale.

1.2. Literature Review

The academic literature on temporary removable barriers at a residential scale is quite limited likely due to the strong presence of proprietary technologies on the market which does not lend itself well to comparative studies (Lankenau et al., 2020). As a result, this literature review will focus more broadly temporary flood protection systems and their evaluation procedures. It is important to note that temporary flood measures can only be as effective as their local flood forecast and warning systems, as without proper communication, temporary measures will likely not be installed properly or on time (Ogunyoye et al., 2011).

A temporary flood protection system is formed by removable flood protection products that can be wholly installed during a flood event and can be removed completely when water levels have receded (Ogunyoye et al., 2011). Some guidelines differentiate these from demountable systems where part of the system is permanently installed and requires additional parts or systems for it to become operational during a flood event. Massolle et al. (2018) utilized a similar concept to differentiate between location-based (requiring some permanent installation) and location-independent flood barriers. Within this document, these two different definitions will be combined to broadly address temporary systems as certain approaches tested fall within these two categories and the academic literature does not always differentiate between the two. Furthermore, these systems are also referred to as flood fighting (Pinkard et al., 2007) or flood mitigation (ANSI, 2020) systems as well, however throughout this document, the term flood protection system will be used.

Biggar & Masala (1998) broadly classified temporary barriers into the following categories based on the underlying technology:

1. Gabion/cellular type
   Prefabricated modular structures (sometimes in metal wiring or plastic) filled with rock, soil or water. The outer structure is often collapsible allowing them to be easily stored between applications and provide protection through their own self-weight (once filled). Examples of these type of structures includes sandbags, gabions, and Hesco Bastions.
2. Concrete or metal removable
   These are prefabricated modular structures made from concrete and metal. These barriers often require heavy machinery to install and specialized connections to make watertight, but are used in a wide range of other practices. They provide protection through their own self-weight, but do not need to be filled. Examples include the Jersey highway barriers and the Portadam.
3. Stop-log dykes
   These types of structures consist of hollow horizontal members lined with gaskets placed between vertical piles. The horizontal units can often be easily removed and stored when not needed. While the installation of the horizontal members is straight-forward, the vertical members must be connected to an existing stable wall or be installed with a concrete foundation. Examples include the GOH DPS 2000 system and the IBS Demountable Flood barrier system.
4. Geomembrane tubes
   These structures use thin membranes to surround air or water that provide a dam to the inundating water. These structures rely on structural anchoring or self-weight to maintain their stability but can often fold down and be stored in-place (or nearby). Examples of these structures include the NOAQ Flood Fighting system and the FlowStop barriers.
5. Modular retaining walls

These structures are often hollow precast concrete blocks that can be filled with sand and stacked to form a self-supporting wall. Similar to the gabion/cellular types, they have been used in a variety of civil work and provide stability through their own self-weight. However, due to their more complex shape, skilled labour is often needed to ensure a stable structure.

6. Fabric foldback
   These structures are essentially reinforced earth structures. They use impermeable sheets between soil layers to improve stability and impermeability. These can be used in conjunction with sandbags to improve their performance or with machine-filling to improve the speed of construction.

Massolle et al. (2018) used a similar classification system, but more broadly classifying them based on the level of pre-installation required for the system (Figure 3). They were also able to include more recent technologies like mobile walls that respond passively to rising water levels and permanently installed membrane structures.

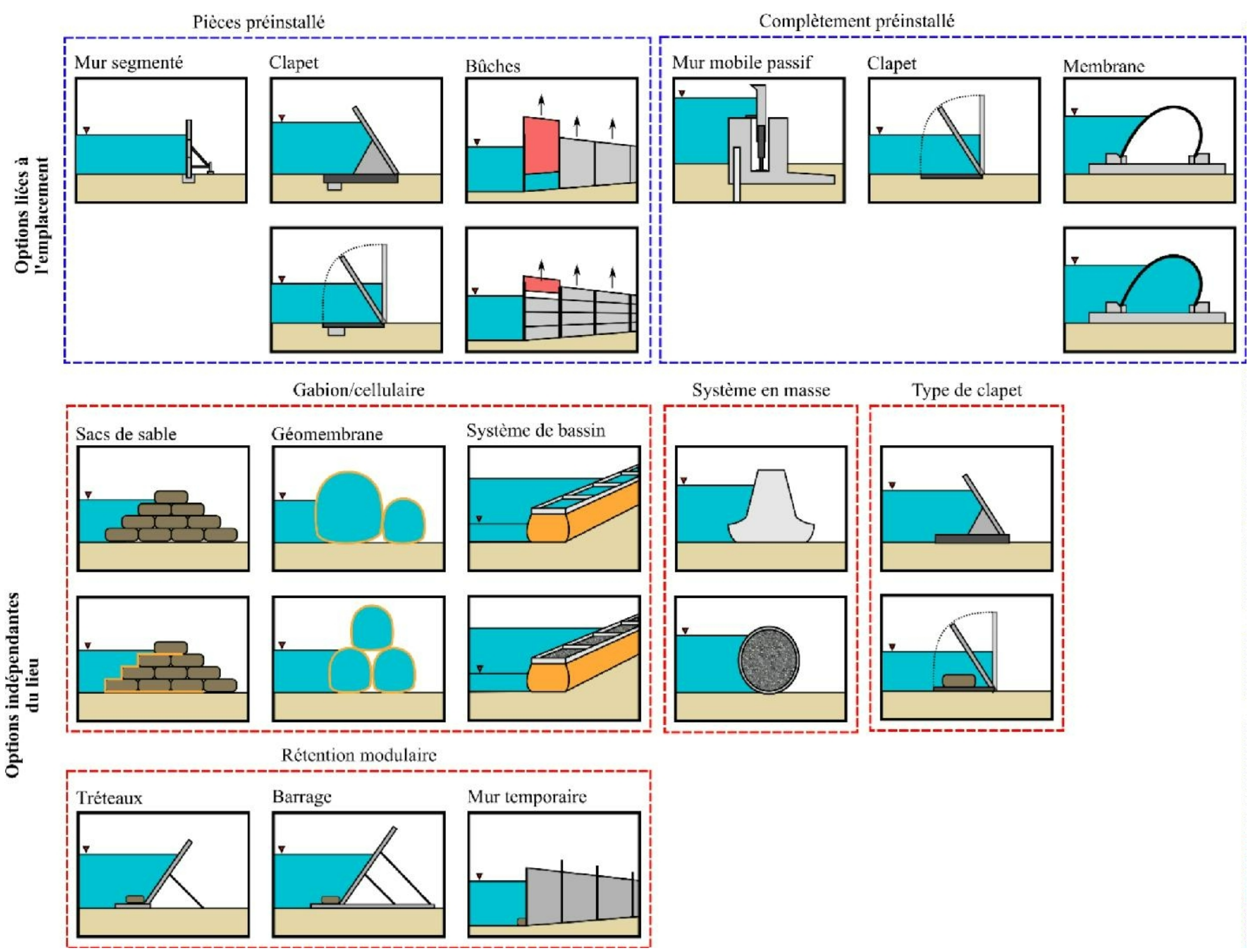

Figure 3. Classification system of perimeter barriers adapted from Massolle et al. (2018) and Biggar & Masala (1998)

The specific application of the various flood protection measures depends on a range of factors including expected loading as well as the type and frequency of flood events. The type of event and structural geometry can influence the forces on the barrier. These forces can include:

1) Hydrostatic (F_{hs})
   The hydrostatic force is the force generated by the hydrostatic pressure acting on the surface of the barrier. The hydrostatic force is proportional to the instantaneous water depth at the surface of the barrier. It can be calculated as a function of the mean water depth, density of water, and acceleration due to gravity.
2) Hydrodynamic (F_d)
   Hydrodynamic forces can be broadly classified by the type of flow: unidirectional or oscillatory (i.e. waves). The forces are caused by the velocity and accelerations of the water particles near the surface of the structure. For unidirectional flow, the hydrodynamic force is proportional to the current velocity and surface exposed to the flow. For oscillatory flow, the local and temporal accelerations of the particles also should be considered.
3) Uplift (F_s)
   Uplift forces are a broad category of forces that act in the vertical direction (countering the weight of the barrier). These can include forces related to hydrostatic and hydrodynamic conditions. The most often considered is the buoyancy force, which is proportional to the volume of fluid displaced by the barrier. If the barrier has a horizontal piece that extends into the moving fluid, a lift force can also arise caused by the pressure change as the fluid moves over the surface. This hydrodynamic uplift force can either be in the positive or negative direction. For barriers placed on permeable surfaces (such as natural turf), uplift forces can also be generated by pore water pressure in the soil or strata under the barrier.
4) Wave Impact (F_v)
   Wave impact forces are a complicated function of the wave conditions and geometry of the structure. When the wave does not break at the structure, the force can be considered a quasi-static load, and hydrostatic forces can be calculated based on the oscillating water surface. In cases where the waves break, often a stochastic process dependent on wave conditions, structural geometry and the slope in front of the structure is undertaken. Further, air can be trapped in breaking wave exerting an impulse load on the barrier several orders of magnitude higher than the hydrostatic and hydrodynamic forces.
5) Debris/Ice (F_i)
   Debris impact forces capture a wide range of scenarios where solid objects entrained in the incoming flood flow impact the structure. The magnitude of the force is primarily determined by the weight of the debris, impact velocity and the debris material. Since the impact load is a stochastic process, assessing plausible impact scenarios is necessary. In the case of ice, there may be an upper limit of loading dictated by the crushing strength of ice.

Figure 4 shows a conceptual drawing of how these forces can act on a barrier dependent on water depth, wave conditions and current. Other forces can also arise that are not captured within the five categories listed above (such as vibrations); however, these are often difficult to assess a priori and may require physical or numerical modelling to properly capture. Aside from any structural or functional damage due to the flood, the performance of barriers are often measured as discharge rate (m^3/h) across the length of the barrier (or the length plus the two sides for opening barriers). The leakage discharge by-passing the barrier can generally come from three places: over the top of the barrier (overtopping, Q), through the barrier (leakage, q), or under the barrier (seepage, S). In the design standards (discussed below), the focus is often on the leakage rate through the barrier as the other two conditions are dependent on the relative overtopping level (often a design scenario that is avoided) and subsurface conditions (site-specific).

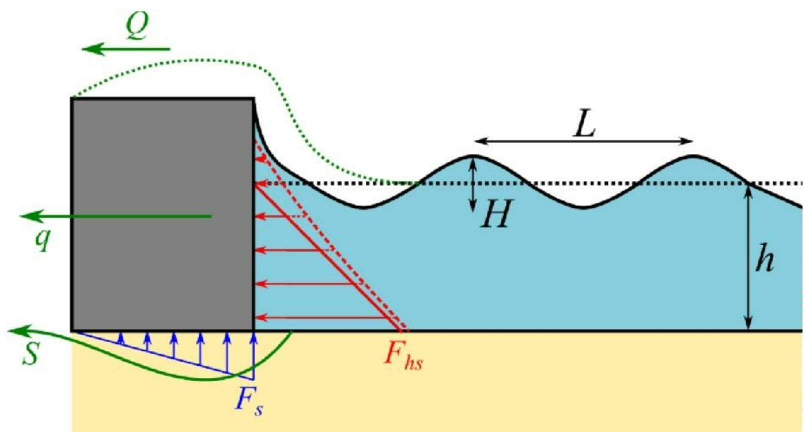

Figure 4. Forces on a flood barrier. H is the wave height, h is the water depth, L is the wavelength, F_{hs} is the hydrostatic force, F_s is the lift force, Q is the overtopping rate, q is the leakage rate, and S is the seepage rate.

Depending on the type of barrier and the forcing mechanisms, the barriers can fail in a variety of ways. Some of the primary modes of failure include:

- Sliding
  Sliding generally occurs for barriers that rely on their self-weight for stability. Sliding occurs when the horizontal forces overcome the frictional forces between the barrier and the bed.
- Overturning
  Overturning occurs when the horizontal or vertical forces induce a rotation of the structure. Again, this usually occurs for barriers that rely on their self-weight for stability; however, it can also be caused by forces inducing large moments on structural members that ultimately fail.
- Overtopping
  Overtopping occurs when the water level exceeds the top of the barrier. As most of the barriers listed here are last lines of defence, overtopping would likely be considered a failure of the infrastructure. This is often a question of design height of the barrier, or flood forecasting to appropriate water depths at the barrier. However, some select barriers may be designed to permit small amounts of overtopping, but the influence of high currents over the crest needs to be considered.
- Erosion
  Flood barriers, by their nature, impeded incoming flows. In the event of high currents and an erodible surface, the influence of scour near the barrier may need to be considered. Scour can result in the undermining and destabilization of the structure that may induce other types of failure or lead to increased leakage rates.

- Puncture
  Puncture is of particular concern to membrane type barriers. Punctures can occur from debris impact or from improper inflation of the membrane. Puncturing inflatable barriers would cause the membrane to lose pressure and deflate reducing its capacity to impede flood waters.
- Durability
  Durability refers to a variety of factors that may influence the long-terms efficacy of the barrier. This could include general wear-and-tear from the mobilization/demobilization of the barriers as well as environmental factors such as UV damage or freeze-thaw cycling. This may be of particular concern for barriers that rely on gaskets or other small pieces that may wear down without being easily identifiable.
- Improper installation
  Barriers are only efficient if they are used as designed and in the appropriate environment. This means that users should be careful when selecting the type and installing the barriers, but also, manufacturers should ensure that the instructions and clear and easy to follow.

In most cases, temporary flood systems are last line of defence in the event of a major flood event (Figure 5). They should not be relied upon for regular protection measure but should only be considered during extreme events where flooding will overtop permanent protection systems (Bramley & Bowker, 2002). The selection of the type of barrier needs to consider not only engineering considerations but also land use, cost, available human resources, and expertise.

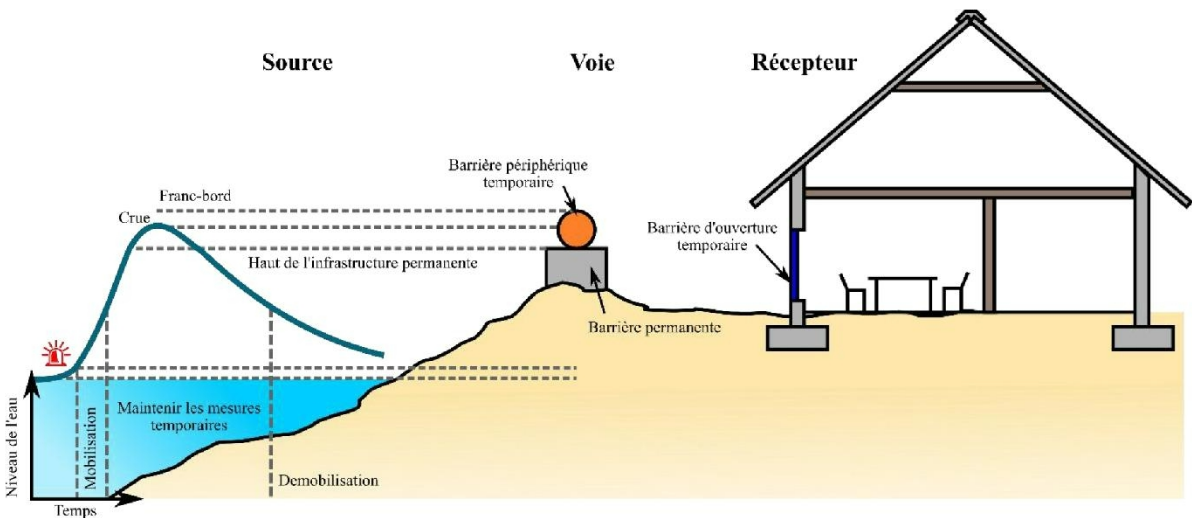

Figure 5. Source-Pathway-Receptor diagram for temporary flood barriers (adapted from Ogunyoye et al. (2011) and Bramley & Bowker (2002)).

The most evaluated temporary flood protection measure in the literature are sandbags due to their widespread use in flood mitigation (McNeil, 2020) as well as in permanent civil constructions (Lohani et al., 2006). They also tend to be used as the reference case to compare the performance of other potential options (Bramley & Bowker, 2002).

One of the key benefits of sandbags is that they show good compressive strength under vertical forcing, even in cases without horizontal confinement (Lohani et al., 2006). This allows them to be relatively easily installed without the support of a secondary or permanent system. Krahn et al. (2007) noted that sand piles under moderate shear loading can provide similar performance to sandbags and sometimes greater performance due to slipping between the geotextile layers (Lohani et al., 2006). However, as loads increase, the strength provided to by the geotextile bag becomes critical. Sandbags are used throughout Canada including extensively in Gatineau during the 2019 floods (McNeil, 2020) and in Winnipeg as a semi-permanent flood defence (Krahn et al., 2007). The configuration of the sandbags is very important to their performance with horizontal rows increasing the overall efficacy of the of the structure (Reeve & Badr, 2003). The inclusion of a waterproof geotextile underneath the structure and folded over the exposed face (sometimes referred to as an apron) also can greatly improve performance (Massolle et al., 2018). However, this can be balanced with reduced friction between the sandbags and bed surface (for some commonly used polyethylene materials) which can contribute to shear failure (Krahn et al., 2007).

The primary challenge around sandbags is related to the labour and time required for their setup. During the 2013 German flood, over 100 000 professional and volunteers were mobilized to transport, fill, and place sandbags (Massolle et al., 2018). In the 2019 floods, several calls were made to volunteers in the Ottawa/Gatineau area to help with sandbag placement. The placement of sandbags is often time-consuming and presents complicated logistics in an already complicated crisis (Figure 6). Furthermore, sandbags are often not reusable and provide significant environmental challenges in their disposal (Molnia, 1973).

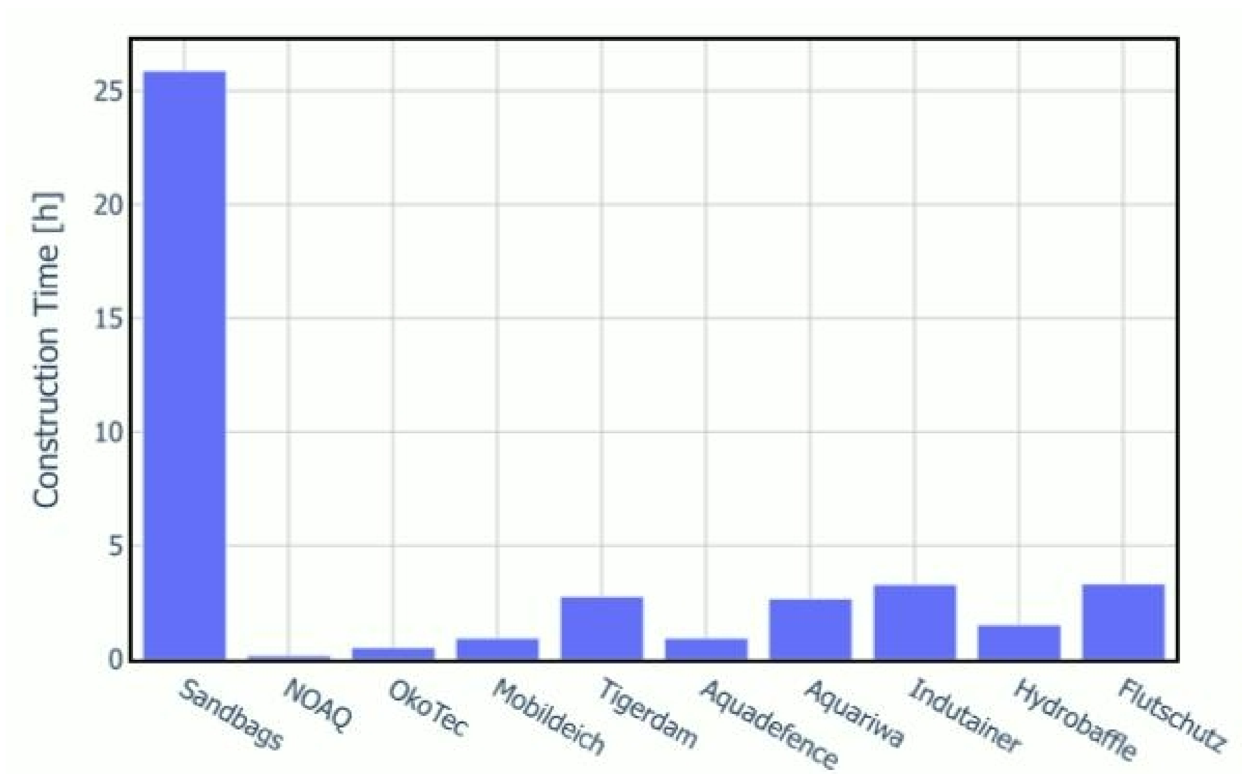

Figure 6. Construction time for 15 m of various perimeter barrier technologies (adapted from Massolle et al. (2018)).

Governments around the world and at various times have explored alternatives to sandbags, including in the United States of America (USA) and the United Kingdom (UK) in 2003 (Ogunyoye et al., 2011; Pinkard et al., 2007). These systems are sometimes also referred to as a Sandbag Replacement System (SRS) in the literature. The objectives of these systems are to improve the constructability time while also being easy to implement and re-useable.

The reported performance of SRSs in the literature is relatively minimal as they are commonly tested in the context of standards to receive certification. Massolle et al. (2018) tested a range of location-independent systems under hydrostatic loading (maximum of 0.6 m) water depth at the Institute for Hydraulic and Coastal Engineering of the Bremen University of Applied Sciences in Germany. The study examined the constructability of the systems as well as their performance, defined by the seepage value (in this case incorporating seepage, leakage, overtopping - a volume per minute per meter of structure). The study found that many of the SRS systems outperformed sandbags (Figure 7) and they were also able to be constructed much quicker. Massolle et al. (2018) noted the importance of the surface below the barrier (in this case, natural turf) on the performance of the different systems.

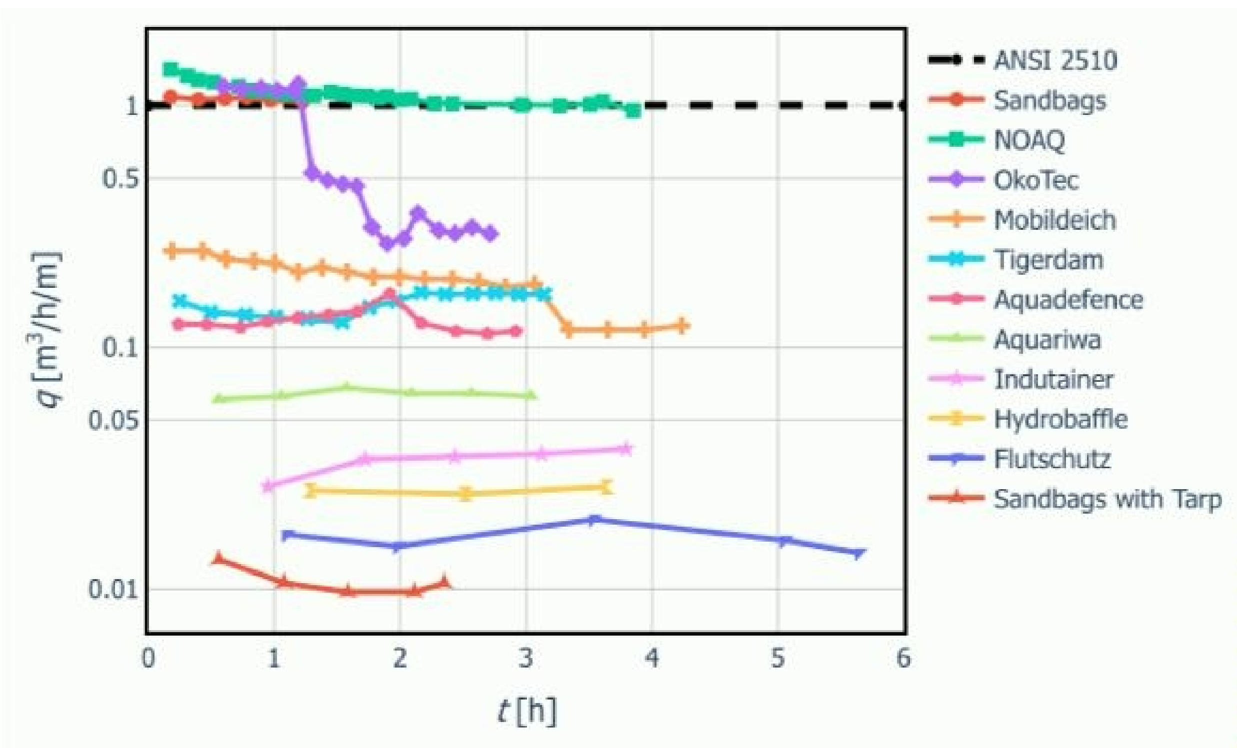

Figure 7. Combined (leakage, seepage, and overtopping) rate for various perimeter barriers (adapted from Massolle et al. (2018)) under a hydrostatic load with 0.60 m water depth.

One of the key challenges in the uptake of these temporary flood barriers has been the perceived safety and economic value of these systems (Lankenau et al., 2020). Kreibich et al. (2011) showed that (for Europe) for flood events that occur at least once in every 10 years that temporary flood barriers have a net economic benefit. For perceived safety, work in both the USA and UK have cumulated in the development of the American National Standards Institute (ANSI) 2510 and the British Standards Institute (BSI) 851188 related to temporary flood barriers. However, it is still unclear how well these approvals are recognized in other countries around the world (Lankenau & Koppe, 2019).

The ANSI standard initially based on a series of lab and field investigations into flood protection barriers by the United States Army Corps of Engineers (USACE) (Pinkard et al., 2007). The lab investigation was performed at the United States Army Engineer Research and Development Center (ERDC) in Vicksburg, Mississippi and the field testing was done at the Vicksburg Harbour. Four different flood protection measures were tested: sandbags, two gabion-style modular units filled with sand (Hesco Bastion and Rapid Deployment Flood Wall), and a wall-style trestle system (Portadam). A summary of the study is shown in Table 1.

Table 1. Summary of lab and field-testing results from Pinkard et al. (2007).

Product	Strengths	Weaknesses
Sandbags	1. Low product cost 2. Conforms well to varying terrain 3. Low seepage rates 4. Can be raised if needed	1. Labor intensive and time consuming to construct 2. Not reusable
Gabion-style (Hesco Bastion)	1. Ease of construction / removal (time and manpower) 2. Low product cost 3. Reusable 4. Can be raised if needed	1. Significant right of way required due to granular fill 2. High seepage rates
Gabion-style (RDFW)	1. Ease of construction 2. Low seepage rates 3. Reusable 4. Can be raised if needed 5. Height flexibility	1. Significant right of way required due to granular fill 2. High product cost 3. Labor intensive and time consuming to remove
Wall-style (Portadam)	1. Ease of construction / removal 2. Low seepage rates 3. No required fill 4. Reusable 5. Limited total right of way required	1. Punctured during laboratory debris impact test 2. Cannot be raised in a typical application 3. Not applicable for high wind use without anchoring

The ANSI 2510 represents the most comprehensive standard in flood protection systems focusing not only on the performance, but also on constructability, reusability, and maintenance (ANSI, 2020). It includes sections related to other flood mitigation measures (such as pumps and valves), but the focus here will be on the hydraulic testing of opening and perimeter barriers.

The standard provides provisions for testing the various system components for issues related to durability and general performance including hydrostatic testing, cycling (deployment and redeployment), impact and wear, aging, as well as environmental stresses, such as temperature, ultraviolet light, and hail. For the perimeter barriers, the barriers are exposed to the testing campaign outlined in Table 2.

Table 2. Test program for perimeter barriers from the ANSI 2510-2020 standard where h is the maximum water depth specified by the manufacturer.

Test	Hydrodynamic Conditions		Duration
	Water Depth	*Other*	
Deployment	N/A	N/A	N/A
Hydrostatic Load	0.30 m	N/A	22 hr
	0.61 m	N/A	22 hr
	h	N/A	22 hr
Wave-Induced Load	2/3h	0.051 – 0.076 m	7 hr
	2/3h	0.152 – 0.203 m	10 min x 3
	2/3h	0.254 – 0.305 m	10 min
	0.8h	0.051 – 0.076 m	1 – 7 hr
	0.8h	0.152 – 0.203 m	10 min x 3
	0.8h	0.254 – 0.305 m	10 min
Overtopping	0.025m overflow	N/A	1 hr
Debris Impact	2/3h	0.30 m diameter log 277 kg mass 2.13 m/s impact 70^{o} impact angle	N/A
	2/3h	0.43 m diameter log 358 kg mass 2.13 m/s impact 70^{o} impact angle	N/A
Current	2/3h	2.13 m/s current (parallel to barrier)	1 hr
Hydrostatic Load	h	N/A	1 hr – 22h

The standard (ANSI, 2020) provides strict requirements on what must be included in the manual regarding material, tools, equipment required, number of people-hours, deployment time, level of expertise as well as a detailed procedure. For performance requirements of the perimeter barrier, the leakage rate should not exceed 0.186 m^3 per meter length per hour and the deflection should not exceed 0.15 m for the hydrostatic tests, the smallest wave-induced loads, current and debris impact tests. The standard defines the characteristic length as the barrier length measured along the center point of the barrier's seal to the ground. For the higher wave-induced loading and overtopping tests, no leakage rate is defined but the barrier should not experience any catastrophic failure, fill loss, or overturning and should not exceed a maximum deflection of 0.15 m.

For opening barriers, the standard only requires that they are exposed to the hydrostatic and debris impact load tests. For all test conditions, the maximum leakage rate is 0.001 m^3 per meter per hour, where the characteristic length is defined as the opening width plus two times the water depth above the opening threshold. The more than two orders of magnitude difference in the allowable leakage thresholds between perimeter barriers and opening barriers is related to potential mitigation measures and susceptibility. Specifically, a perimeter barrier is installed around the perimeter of a building and pumps can often be installed to control water levels between the barrier and the building. Three 1-inch pumps or two 2-inch pumps would be sufficient to manage the leakage around a typical 140 square meter (1500 square foot) home if the leakage does not exceed 0.186 m^3 per meter length of barrier per hour. For an opening barrier the threshold is much less. It is assumed that the water leaking through the opening barrier is entering the building where there is no ability to install pumps. It is assumed that any leakage would need to be managed with absorbent materials such as towels. Assuming a 1.5 m seal length and that a single towel can absorb 1 to 1.5 kg of water, 8 towels would absorb the water from a leakage rate of 0.001 m^3 per meter of seal per hour for a 5-8 hour period before needing to be replaced.

The ANSI 2510 thresholds as described in the previous paragraph are suitable points of reference when discussing reasonable allowable leakages rates for perimeter and opening barriers. As such, they will be the reference for comparison within this report. The research team determined that the regular waves defined by ANSI 2510 were not the preferred approach to assess resiliency to wave action. Generally regular waves are only tested in a laboratory facility until reflections interfere with the test area. Reflections can result in undesired wave interference. For this reason, in this series of experiments, more realistic irregular waves were used to determine barrier resiliency to waves. It was also decided to use a lower energy impact test than the ANSI 2510 standard. In ANSI 2510 two impacts at 600 J and 800 J respectively were used for impacts tests, for this study impact tests of 140 J using a 0.30 m diameter and 277 kg log at a speed of 1.0 m/s were completed. These experiments seek to understand what types of flood protective measures are useful for Canadian homeowners as well as inform the future development of a Canadian standard or flood barriers. We are not assessing any products against any current or future standards.

1.3. Research Needs

Based on the literature review proposed above, the following research needs have been identified:

- More data is needed regarding failure modes of the building envelope and openings in real-world conditions. This is particularly relevant in non-European contexts as building standards and materials vary widely throughout the world.
- Loading conditions that lead to failure of temporary barriers needs to be further explored. Limited studies have addressed the primary causes of failure; hence, limited data exists on the loading that can cause failure.
- Research is needed into the regional specific loading and stresses (such as in coastal, urban and rural settings, and/or temperature changes, ice, salinity, etc.) that may impact the performance of temporary barriers. Current design standards globally have mostly been focused on temperate and riverine contexts.
- More data is needed on the performance of temporary residential opening barriers as the literature has primarily focused on perimeter barriers.
- Standards for temporary residential barriers need to be more widely shared and be relevant to the context in which they are used to ensure the confidence of the general public.

1.4. Objectives

The long-term goal of the project is to provide Canadians with standardized temporary flood protection measures that will improve the overall resilience of our communities. Within this testing program, the aim was to develop an experimental protocol that fits with Canadian construction standards and evaluate the current limitations of the protocol. The specific objectives of the project include:

1) Examine the efficacy of current Canadian building standards (NBC, 2020) in flood protection without any temporary barriers present.
2) Evaluate the performance of several classes of temporary residential opening flood barriers under various loading conditions.
3) Observe how temporary opening barriers function with and without their infrastructure (such as doors and windows).

This report is a preliminary look at the results of the experiments that took place between October 2024 and January 2025 at the NRC in Ottawa, Ontario. The report is separated into the following sections:

- Section 2: Experimental Setup which outlines the setup of the experimental facilities, the instrumentation and temporary opening barriers used, as well as the experimental protocol.
- Section 3: Analysis which looks at the different analysis procedures used to interpret the output from the instrumentation.
- Section 4: Results which interprets the preliminary analysis of the data compiled during the testing program and discusses the implications.
- Section 5: Conclusions and Recommendations which summarizes the principal conclusions and recommendations for next steps.

2. Experimental Setup

2.1. Laboratory Facilities

The experiments were performed in the multi-directional wave basin at the National Research Council of Canada (NRC) in Ottawa, Canada. The wave basin is 30 m × 36 m × 3 m with a multi-directional wave generator on one side and a dry pit on the opposite side. The building envelope (hereafter referred to as the superstructure) was placed on a raised reinforced concrete pad (0.254 m high). The platform was surrounded by a 1:8.9 slope down to a flat surface. In front of the wave generator, a slope of 1:9.66 raised the bed up 0.75 m to the flat surface. The zero-reference elevation was considered to be at the elevation of the concrete pad.

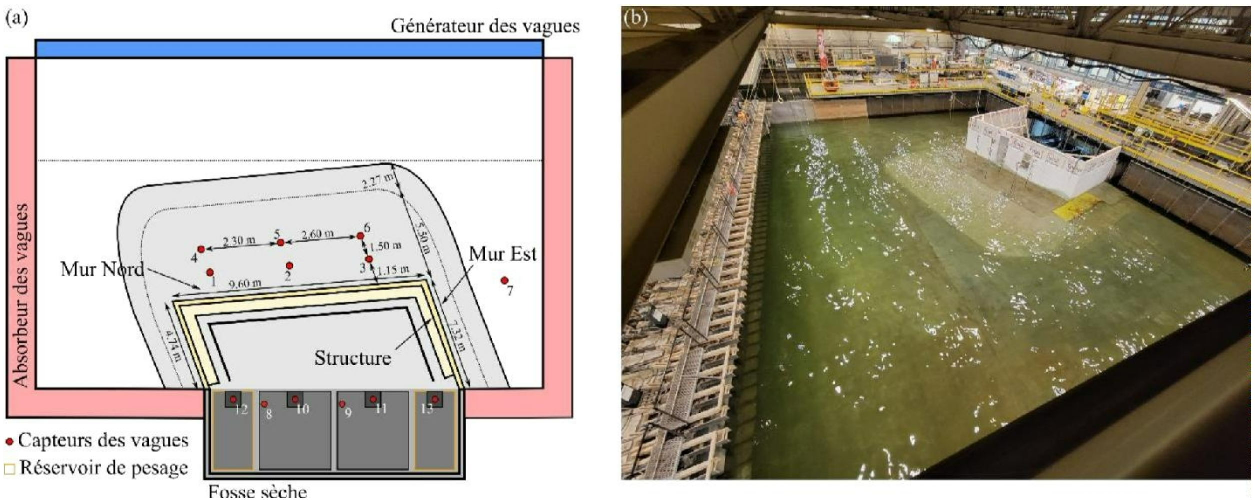

Figure 8. Plan view of the experimental facilities at the NRC. (a) Conceptual sketch of superstructure and instrument positions; (b) photo of Phase 1 testing of waves.

The superstructure was connected to the sidewalls of the dry pit to ensure that water infiltrating the internal area of the superstructure was only through the openings or the superstructure itself. The superstructure was attached to the sidewalls through two rows of 19 mm diameter threaded inserts and sealed with silicone.

The experiments were performed in two phases. The first phase was to evaluate the infiltration rate of a standard Canadian residential home construction. The second phase focused on the performance of the individual temporary residential opening barriers. For each case, the superstructure was setback 0.15 m from the edge of the slope on the two sides.

2.2. Superstructure

2.2.1. Phase 1 – Residential Home

The superstructure in Phase 1 was built to represent a common residential dwelling following the National Building Code of Canada 2020 (NBC, 2020). The structure was built with 0.038 cm × 0.14 m kiln dried SPF lumber. The cross-section of the wall component is shown in Figure 9a. The floor joists were placed on 0.038 m × 0.14 m sill plates and attached to concrete platform with 13 mm diameter anchor screws every 1.20 m (as well as at each corner and at the openings). A rim joist (0.038 m × 0.235 m) was placed on the sill plate. Wall studs were placed at approximately 0.41 m intervals and were nailed according to the National Building Code of Canada 2020. One door opening (0.285 m above the platform) and one window opening (0.735 m above the platform) was constructed in the building envelope.

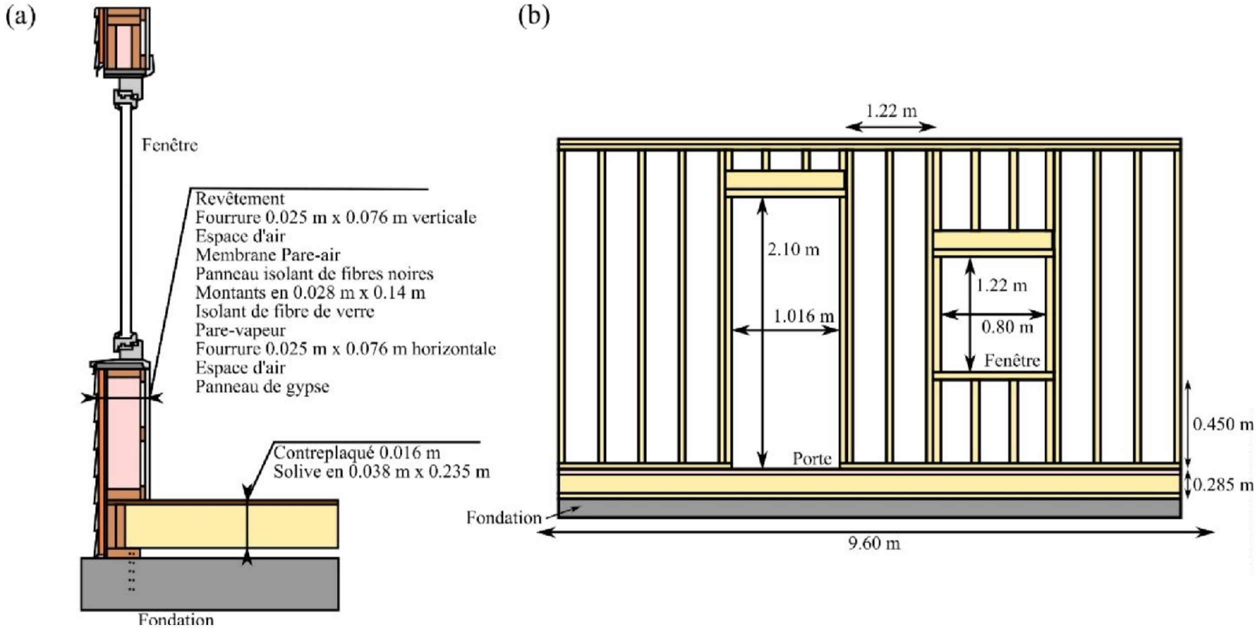

Figure 9. Phase 1 superstructure based on Ontario Building Code. (a) Cross-section of the superstructure; (b) front view of the superstructure.

The floor joists (0.038 m × 0.235 m) were connected to tie back plates 1.67 m behind the building envelope. Vertical braces were placed approximately every 1.20 m connecting the top plates to the tie back plates (Figure 10b) and aligned with floor joists. The vertical braces were connected to top plates with four 65 mm nails. The wood frame was covered with 11 mm plywood sheathing and the floor was covered with 16 mm plywood. The interior of the wall was constructed using the cross-section presented in Figure 9a. The exterior cladding was only placed up to a maximum height of 1.95 m (Figure 10b).

Figure 10. Construction of the Phase 1 superstructure. (a) Framing of superstructure; (b) superstructure with insulation and support structure installed; (c) superstructure with exterior cladding being installed; and (d) completed superstructure during testing.

2.2.2. Phase 2 – Opening Barriers

Phase 2 was intended to focus exclusively on the performance of the temporary residential opening barriers. The experiments were performed in two facilities: the multi-directional wave basin (MWB, same facility as Phase 1) and the Ice Tank (IT). The experiments in the MWB were tested with hydrostatic, debris impact, and wave loading. The experiments in the IT were tested with hydrostatic loading and debris impacts.

Multidirectional Wave Basin (MWB)

To avoid any influence of the superstructure on the opening barrier performance, the structure was designed and reconstructed to be rigid and impermeable to water (the residential home from Phase 1 was removed and rebuilt fit for purpose). The structure was built with 0.038 cm × 0.14 m pressure-treated wood. The cross-section of the wall component is shown in Figure 11a. The wall frame was placed on 0.038 cm × 0.14 m sill plates and attached to concrete platform with 13 mm diameter anchor screws every 0.40 m (as well as at each corner and at the openings). Wall studs were placed at approximately 0.30 m intervals and were nailed according to the National Building Code of Canada 2020.

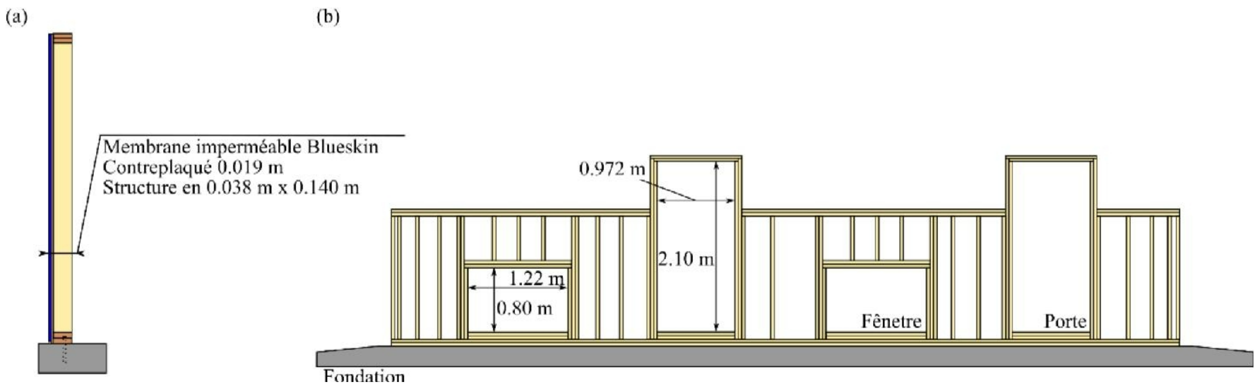

Figure 11. Conceptual drawing of Phase 2 structure. (a) Cross-section of the superstructure; (b) front view of the superstructure frame.

Two door and two window openings were placed 0.15 m above the concrete platform. All the openings were at the same height above the concrete platform to ensure the barriers were exposed to the same conditions. The wood frame was enclosed with 19 mm plywood sheeting and covered with an impermeable membrane (Blueskin WP200). Figure 12 shows the evolution of the construction of the impermeable structure within the NRC MWB basin.

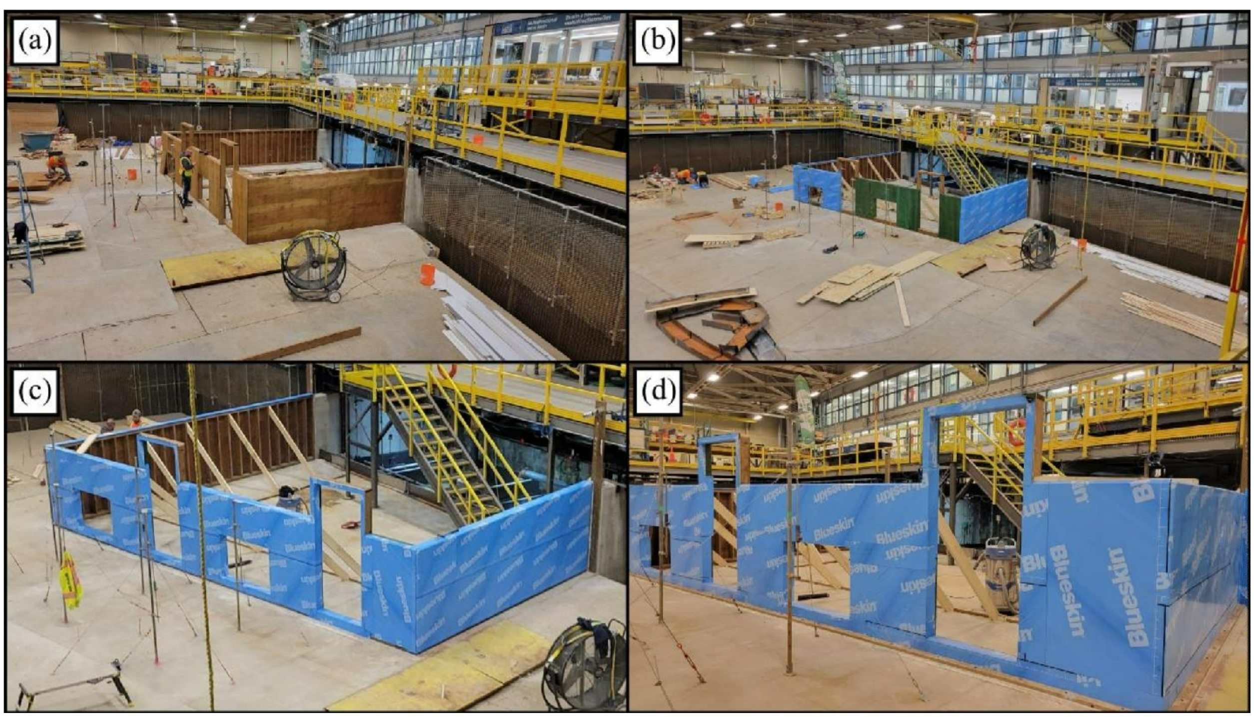

Figure 12. Construction of the Phase 2 impermeable structure. (a) Wood framing of structure; (b) placement of the waterproofing membrane; (c) completed waterproofing membrane; and (d) door and window openings.

Ice Tank (IT)

A new superstructure was built within the NRC Ottawa Ice Tank facility (IT) which had a similar design to the Multidirectional Wave Basin (MWB) Phase 2 superstructure. However, the IT superstructure was designed to hold water in the interior (the inverse of the MWB) and could support deeper water depths. The structure was built on a 0.20 m thick concrete pad with an area 4.096 m by 4.096 m. The IT superstructure itself was 3.696 m by 3.696 m with three internal reservoirs – i.e. the ability to test up to three barriers at once all to their own unique water level. Images from the testing within the facility are shown in Figure 13. One small reservoir had a window (Figure 13c), and another small reservoir had a door (Figure 13d), while the larger reservoir had both as shown in Figure 13a and Figure 13b or illustrated in Figure 14. The water level in each reservoir was maintained by an automatic valve.

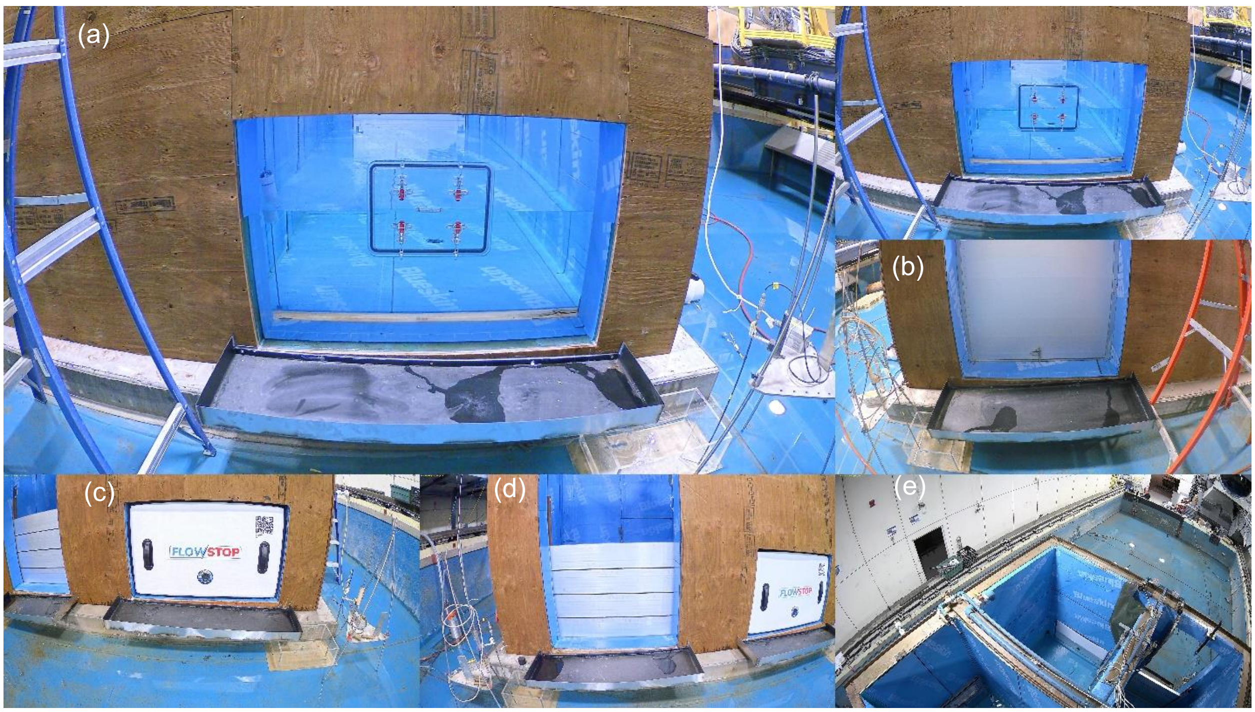

Figure 13. Images of the NRC Ottawa Ice Tank facility during Phase 2 testing

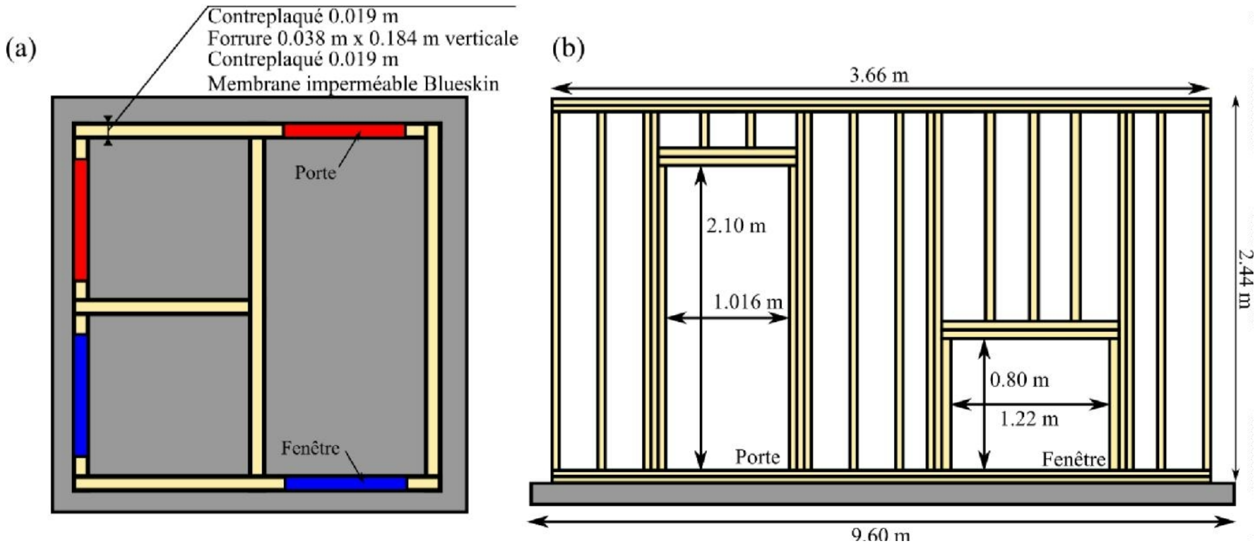

Figure 14. Conceptual drawing of Phase 2 NRC Ice Tank facility. (a) Top view of individual reservoirs (water was placed within the structure). (b) Side view of the structure (shown on the left side of top view).

The structure was built from 0.038 m × 0.184 m SPF pressure treated lumber according to the 2020 version of the National Building Code (NBC, 2020). The walls were clad with 0.019 m plywood on the interior and exterior. The interior wall was covered in the impermeable Blueskin membrane. The wall sill plates were connected to the concrete foundation with 13 mm diameter anchor screws.

2.3. Instrumentation

2.3.1. Leak Collection and Measurement

The main measurement of performance was the leakage rate through either the residential home (Phase 1) or through the opening barriers (Phase 2). The leakage rate was measured using a catch basin system illustrated in Figure 15 and shown in Figure 16. In Phase 1 the leakage was collected from three locations. The first, basement leakage, was collected along the entire 21.37 m perimeter of the model home from the concrete foundation up to the floor package, 0.285 m above the foundation. The water accumulated on the floor of the model home and eventually collected within two tanks within the dry pit where it was measured as a single leakage value. The second location measured leakage through the window and door openings along the north wall and was collected in a 4.41 m long catch basin indicated in green in Figure 15. The catch basin was attached to the floor package which was installed 0.285 m above the foundation. A piece of plywood was used to connect each end of the catch basin to the wall of the model home as shown in Figure 16. The plywood piece was sealed with silicone. The third location where leakage was measured was along the east wall. The 4.51 m long catch basin is indicated in orange in Figure 15. The east wall catch basin was also attached to the floor package, 0.285 m above the foundation, and sealed to the wall with plywood. The blue sections in Figure 15 indicate the gutters running from the north and east catch basins towards two separate tanks within the dry pit. The gutters from the north catch basin are also shown in Figure 16.

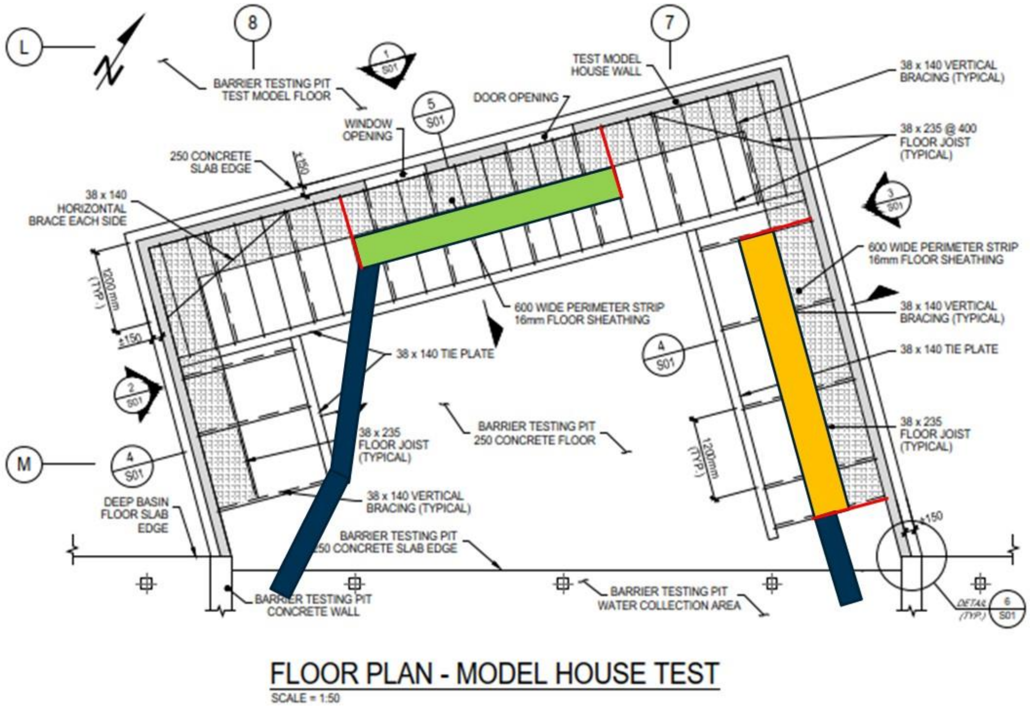

Figure 15. Catch basin system for measuring leakage rates for Phase 1. In green we have the catch basin for the door and window openings; In yellow we have the catch basin for the east wall.

The three sections tell us something different about water ingress into the home. The basement leakage is below the floor package and represents water that will generally end up in the basement. This is where most water will accumulate however, if the space is unfinished and valuables are elevated damages from basement flooding can be limited. It should be noted because the two floor sections only cover 8.92 m of the 21.37 m perimeter of the structure the remaining 12.87 m of 1st floor leakage will also be captured in our basement data as the leakage falls off the floor and onto the concrete slab. It should however be noted that the 1st floor leakage through the wall (> 0.285 m) is much less than the leakage defined as basement (< 0.285 m) because the leakage is dominated by the sill plate connection to the foundation.

There are two sections examined on the first floor. For these two locations the water is assumed to be arriving on finished materials and the potential for damages and financial losses is high. The first measurement location is the openings which captures a window and a door. Those openings dominate the leakage for this location. The second location is the east wall, this is simply a standard wall section which is studied to see the penetration through a wall cavity during flood conditions. It is representative of the other straight wall sections within the model.

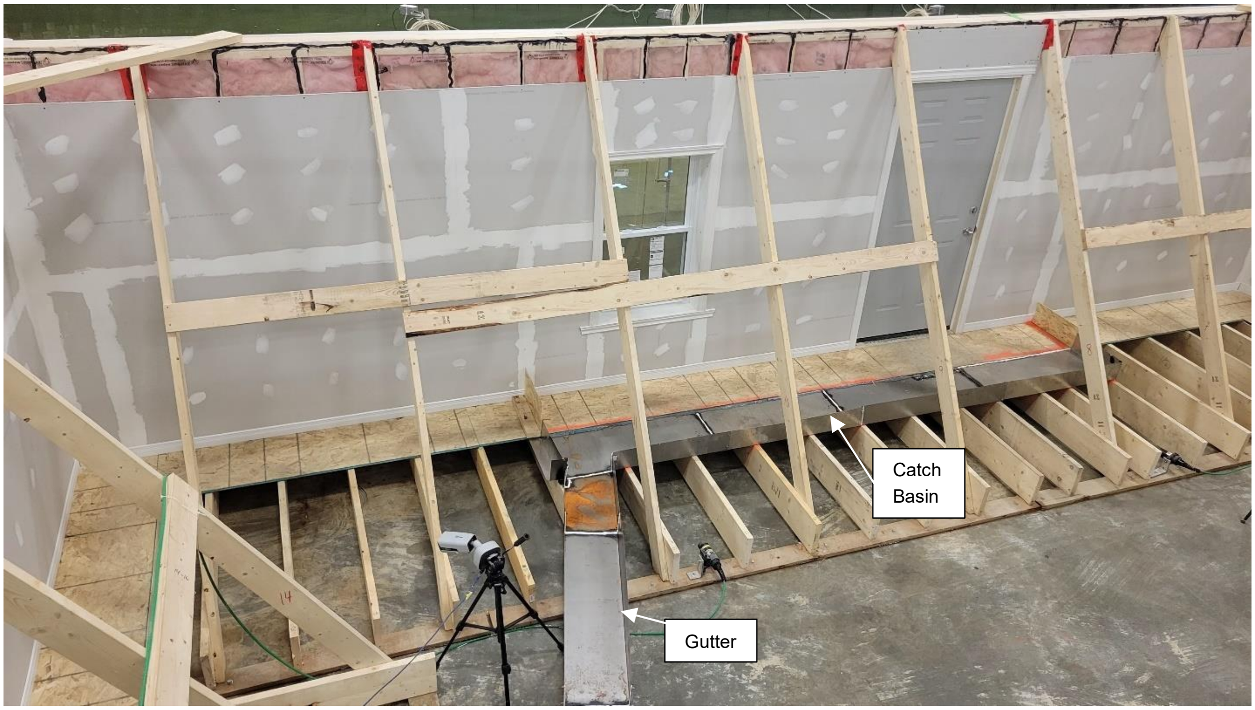

Figure 16. Catch basin system for measuring leakage rates from the door and window openings during Phase 1. A gutter leads from the catch basing towards the dry pit.

Leakage through the openings was conveyed by gutters to the tanks within the dry pit for measurement. Capacitance-type water level gauges were placed within each tank to measure the water depth. With the known cross-section of the tanks, the volumetric change rate was calculated (giving flow/leakage rate). Due to a relatively large difference in expected leakage rates between the different technologies, a two-tiered system was used with a smaller tank being able to capture lower leakage rates and a larger tank to capture the higher rates. When the smaller tank was filled, it overflowed into the larger tank allowing for a continuous measurement of the total leakage rate as shown in Figure 17. Two of the four large tanks were weight tanks, so instead of measuring the water level, the weight of the water was measured, and the volume was inferred based on a density of fresh water of 1000 kg/m^3.

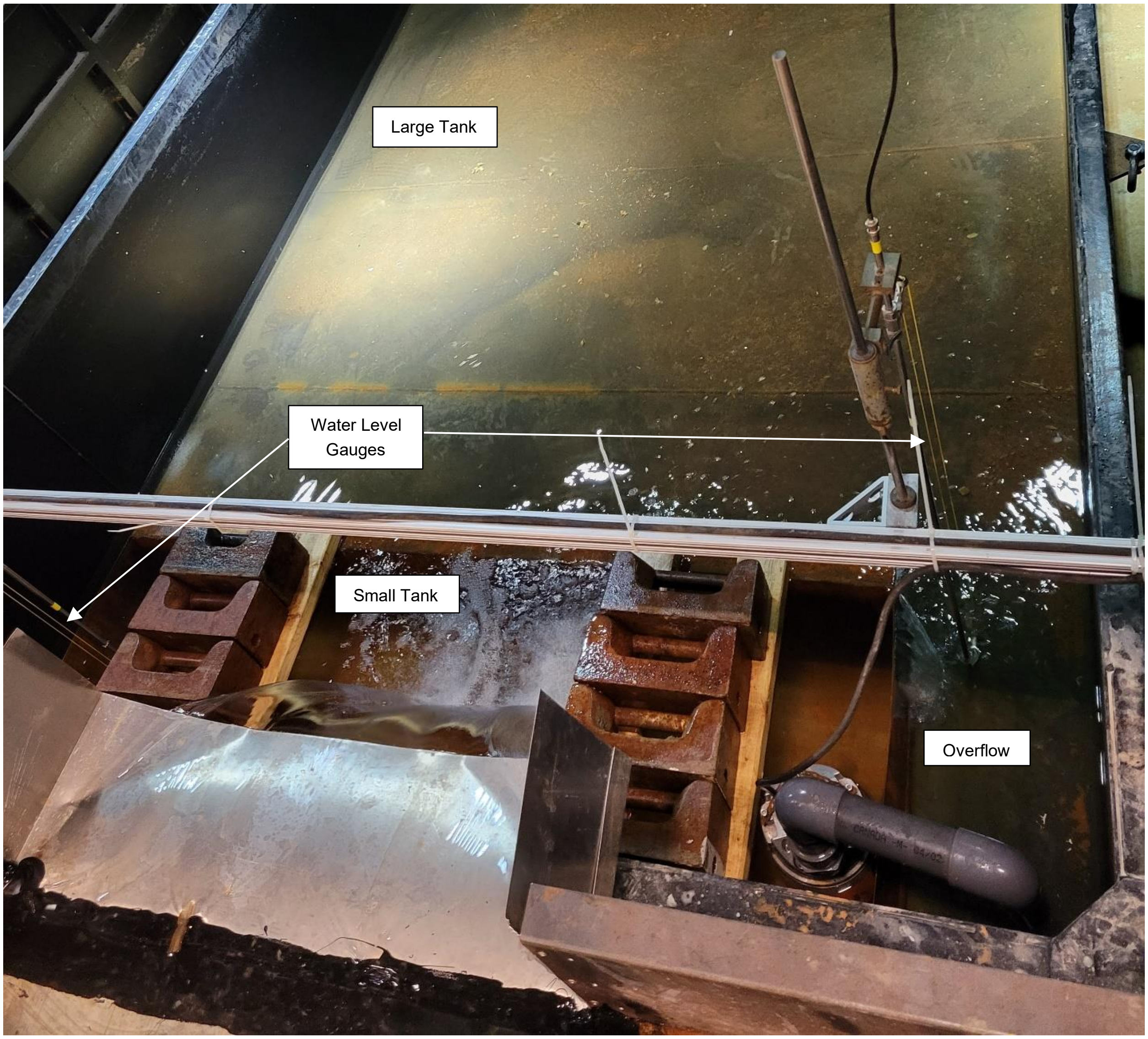

Figure 17. Leakage rate measuring tanks within the dry pit for Phase 1.

In Phase 2 testing there were four different leakages rates measured, one for each of the openings in the superstructure. There were two door openings with the catch basins illustrated in green in Figure 18 and two window openings with the catch basins illustrated in orange. Similar to Phase 1, a gutter ran from each catch basin to a small tank in the dry pit for measurement. The measurement tanks for Phase 2, shown in Figure 19, were smaller than for Phase 1 to account for the lower expected leakage rates for some barriers.

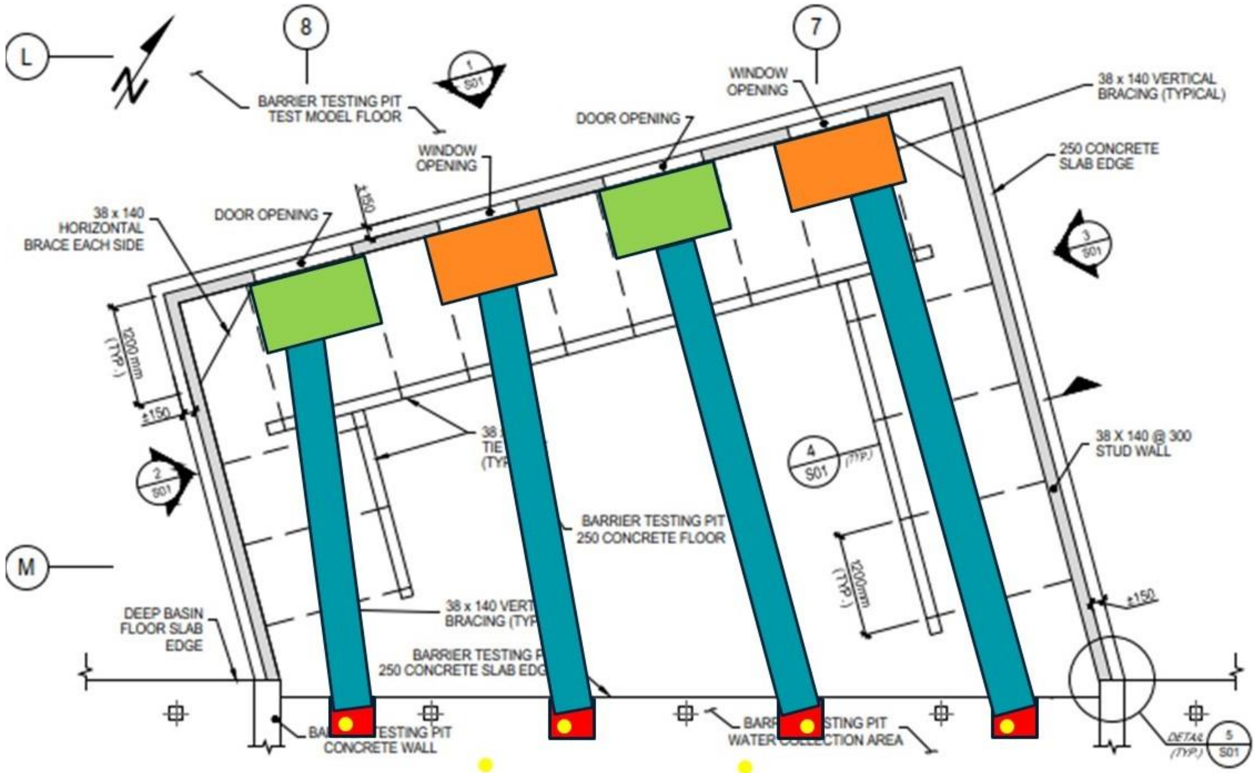

Figure 18. Catch basin system for measuring leakage rates for Phase 2. In green we have the catch basins for the two door openings, in orange we have the catch basin for the two window openings.

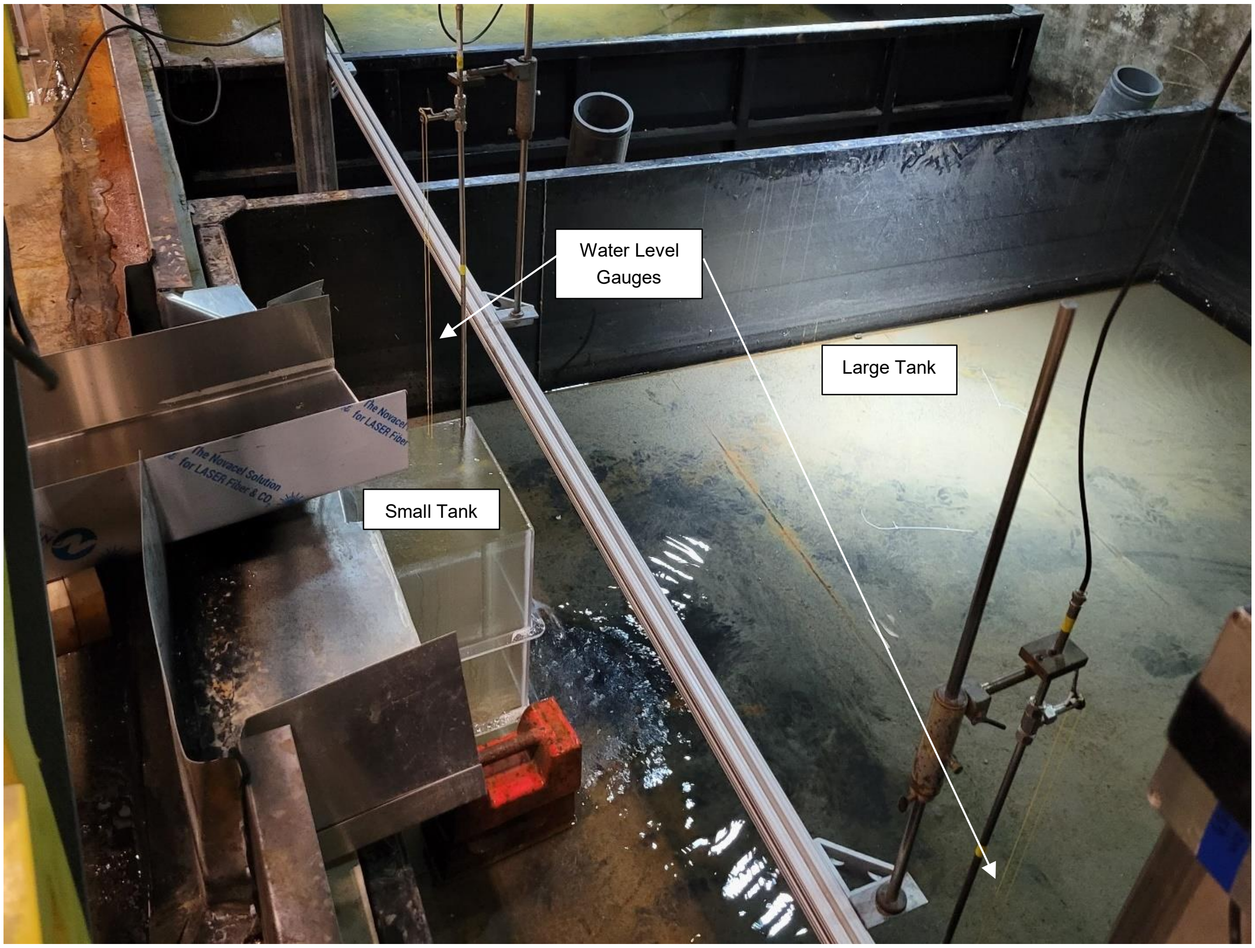

Figure 19. Leakage rate measuring tanks within the dry pit for Phase 2.

2.3.2. Waves

Six water level gauges were placed in front of the structure to measure the incident wave energy. These capacitance type water level probes operated by sensing the change in capacitance that occurs as a portion of the insulated wire become wetted. The output was directly proportional to the percentage of the wire that was wetted, regardless of whether the wetting was continuous or intermittent (as in the case of splash or spray). The water level probes were calibrated by changing their elevation with respect to a fixed water level. The probes feature a highly linear response, with calibration errors typically less than 0.5% over a 200 mm calibration range. This error represents an accuracy of ± 1 mm, and the data was acquired at 50 Hz.

The wave gauges were aligned with the front face of the structure at an offset distance of 1.15 m and 2.65 m from the front wall (Figure 8). The lateral distance between the gauges (running parallel to the front face) was 2.30 m and 2.60 m. WP7 was placed to the side of the structure and was used as the reference water level gauge and set to zero when the water was at the top of the foundation. Video cameras (Table 3) were placed around the facility to monitor leakage rates as well as failure modes, and still photography was taken to highlight key observations.

Table 3. Camera specifications.

Camera Name	Manufacturer	Model	Resolution	Frame Rate (fps)
MWB #1	Sony	SNC-RX570N	640x480	30
MWB #2	Sony	SNC-ER520	720x480	30
MWB #3	Sony	SNC-RX570N	640x480	30
East Door	Bosch	Dinion IP 5000i IR	1920x1080	30
West Door	Bosch	Dinion IP 5000i IR	3072x1728	30
East Window	Bosch	Dinion IP 5000i IR	3072x1728	30
West Window	Bosch	Dinion IP 5000i IR	3072x1728	30
Dry Pit	Sony	SNC-VB632D	1920x1080	30
IT #1	Bosch	Dinion IP 5000i IR	1920x1080	15
IT #2	Bosch	Dinion IP 5000i IR	1920x1080	15
IT #3	Bosch	Dinion IP 5000i IR	1920x1080	15
IT #4	Bosch	Dinion IP 5000i IR	1920x1080	15
IT #5	Bosch	Flexidome IP starlight 8000i	1920x1080	25
IT #6	Bosch	Flexidome IP starlight 8000i	1920x1080	25

2.3.3. Ice Tank (IT)

The measurement systems deployed in the Ice Tank (IT) were similar to those in the Multidirectional Wave Basin (MWB). Since waves were not considered in the IT, only one water level gauge and one camera were placed in each reservoir to measure the still water level. Each opening had a conveyance tray and catch basin for measuring leakage, similar to those used in the MWB. The flood barrier products tested in the IT were expected to have lower leakage rates so only a small catch basin with one water level gauge was used to measure the flow rate for each opening.

2.4. Opening Barriers

A range of opening barriers were tested in Phase 2 of the experiments. For each run of the experimental protocol in the MWB facility, barriers for two doors and two windows were tested. Figure 20 - Figure 23 show the barriers for each of run of the experimental protocol. The barriers were installed according to the specifications described in the guidance document provided with the product. An effort was made to follow the specifications exactly to try and represent (as close as possible) the installation that would be achieved by the general population or a professional without specialized training. Since the water proof Blueskin surface is different than a concrete foundation, suppliers were contacted to see if any modifications should be made to their installation procedures or hardware as a result. As a result of this inquiry, the Flow Stop barriers shown in Figure 20 (b) and (d) as well as Figure 23 (a) were installed after applying non-skid tape to the opening where the barriers were installed; RS Stepanek shown in Figure 21 (a) was fixed to the structure using lag bolts rather than those provided; and the Aqualock window protector shown in Figure 23 (c) was installed onto a wood frame which was adhered to the Blueskin with mechanical fasteners and sealed with silicone. Note that the performance and results for these barriers apply for this specific application, and may differ from those when installed on another surface (such as directly on the concrete foundation). A brief description of the barriers is provided in Table 4, for a more detailed description, please see the supplier's technical specifications.

Figure 20. Opening barriers deployed in the MWB in Phase 2 – first set of tests: (a) plywood; (b) Flow Stop full-sized cushion; (c) sandbags; and (d) Flow Stop regular cushion.

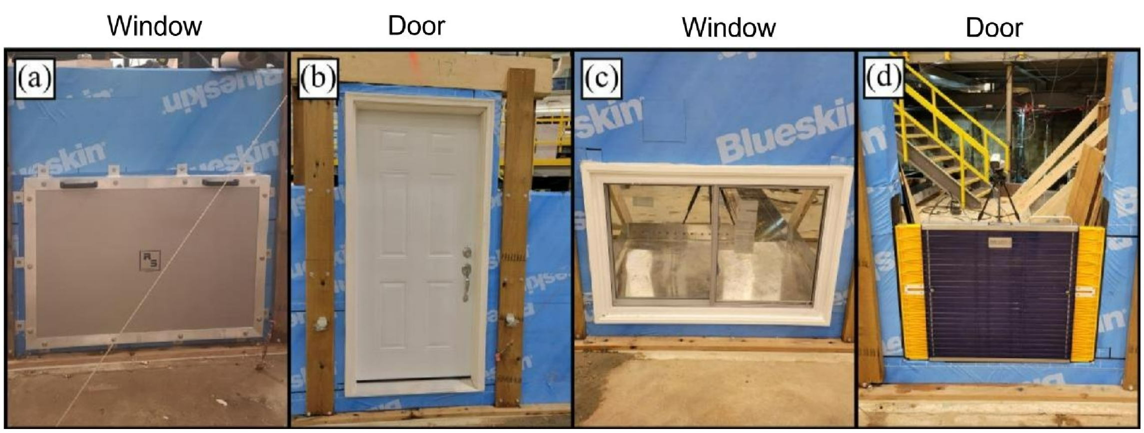

Figure 21. Opening barriers deployed in the MWB in Phase 2 – second set of tests: (a) RS Stepanek; (b) Standard Door; (c) Sliding Window; and (d) DamEasy.

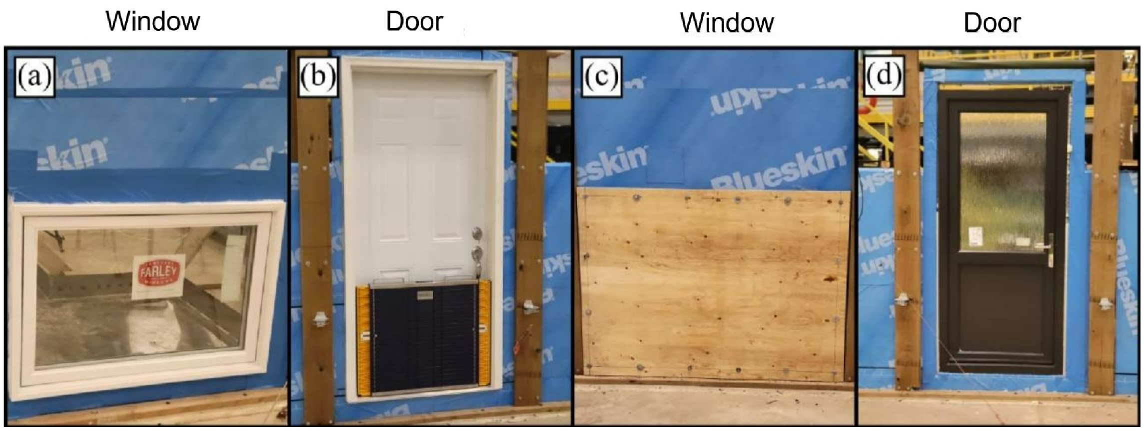

Figure 22. Opening Barriers deployed in the MWB during Phase 2 – third set of tests: (a) Awning window; (b) Standard Door with DamEasy; (c) Sliding Window with plywood; and (d) Stormmeister Flood Resistant Door.

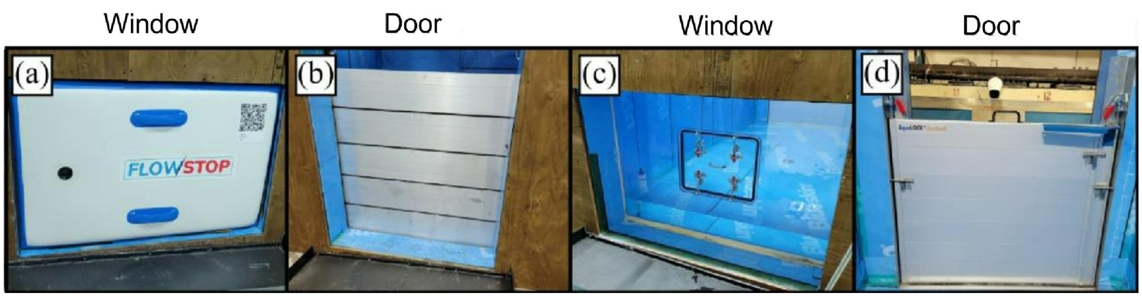

Figure 23. Opening barriers deployed in the IT in Phase 2: (a) Flow Stop full-sized cushion; (b) Stormmeister Rapid Assembly Log type Barrier; (c) Aqualock Window Protector; and (d) Aqualock Quickwall.

Table 4. Description of the various opening barriers used in the experiments.

Type of Opening	Type of Barrier	Company	Model	Test Facility	General Description
Window	Plywood			MWB	19 mm pressure treated plywood. Connected to the exterior of the superstructure with sixteen 65-mm nails.
	Sandbag			MWB	Polyethylene sandbags with an approximate size of 40.6 × 50.8 cm when filled. Sandbags placed in a double row creating a perimeter around window.
	Window	Farley	Series 4200 Double Slider	MWB	A standard double slide window with a vinyl frame. Double-paned 3 mm annealed glass (0.538 m × 0.652 m) with argon gas fill.

	Window	Farley	Series 5000	MWB	A standard top-hinged awning window with a vinyl frame. Double-paned 3 mm annealed glass (1.065 m × 0.646 m) with argon gas fill.
	Membrane	Flow Stop	Full-size cushion	IT	A high-density polyvinyl chloride (PVC) membrane connected using a drop stitch method with polyester threads. Completely covers the opening of the window.
	Covering	Aqualock®	Window Protector	IT	A window cover made of solid acrylic glass (0.02 m thick). The cover has a 0.30 m × 0.40 m cut-out in the center.
	Covering	RS Stepanek	4-sided Window Cover	MWB	A window cover, 2.5 cm thick, fixed to a permanent, 4 cm by 6 cm, rectangular tube frame. The cover and the frame both have 14 attachment points. The frame is sealed to the structure with an adhesive product and the cover is sealed to the frame with a 7 mm thick and 6 cm wide foam gasket.
Door	Door	Masonite	Wood Edge Steel Frame	MWB	Standard 36-inch left hand inswing pre-hung door. The door was locked with the deadbolt during testing.
	Covering	DamEasy®	Flood Barrier	MWB	A modular plastic flood barrier with an inflatable seal to seal two sides. Requires an adhesive filler to seal the bottom side and corners of the barrier.
	Membrane	Flow Stop	Full-size cushion	MWB	A custom-built high-density polyvinyl chloride (PVC) membrane connected using a drop stitch method with polyester threads. Completely covers the opening of the door and seals to all four sides.
	Membrane	Flow Stop	Regular cushion	MWB	A custom-built high-density polyvinyl chloride (PVC) membrane connected using a drop stitch method with polyester threads. Seals to three sides covering a portion of the opening.

	Flood-resistant Door	Stormmeister®	Single uPVC Flood Resistant Door	MWB	A unplasticized Polyvinyl chloride (uPVC) door with Stormmeister® Active Flood Seal which provides flood protection through a chamber-gasket system which seals only when exposed to sufficient water depth.
	Covering	Aqualock®	Quickwall	IT	A custom-built anodized aluminum barrier slatted panel system that can be within or in front of openings with angle brackets. Seals to three sides covering a portion of the opening.
	Log-type	Stormmeister®	Rapid Assembly Flood Barrier	IT	A system of 5 hollow aluminium logs each 110 cm wide, 20 cm high and 5 cm thick. Each log has a 1 cm thick foam gasket along the full bottom except the bottom log where the foam is 5 cm thick. The mounts for the logs include two C-channels which are permanently installed on each side of the opening to be protected and a base plate. The C-channels have a foam gasket along side of the channels attached to the building. The gaskets are 1 cm thick and 4.5 cm wide. The logs are fixed into the C-channels using wooden wedge pieces.

2.5. Experimental Protocol

2.5.1. Phase 1 – Residential Home

The Phase 1 experiments took place over a six-day period. Between test series, the water level was left the same as the end of the previous test series. The test series were separated so that they could be reasonably completed within an eight-hour workday. Leakage rates measurements were averaged over a 15-minute period and were measured continuously over a test series.

Table 5. Phase 1 experimental testing protocol.

Test Series (TS)	Water Level [m]	Duration [h]	Significant Wave Height [m]	Peak Wave Period [s]	Debris Mass [kg]	Debris Impact Velocity [m/s]
A	0.05	0.50				
	0.10	0.25				
	0.20	0.25				
	0.285	22.00				
	0.335	0.50				
	0.385	0.25				
	0.485	0.25				
	0.585	1.00				
B	0.285	0.25				
	0.285	0.67	0.025	3.00		
	0.285	0.67	0.05	3.00		
	0.285	0.67	0.10	3.00		
	0.285	0.25				
	0.585	0.25				
	0.585	0.67	0.05	3.00		
	0.585	0.67	0.10	3.00		
	0.585	0.67	0.15	2.50		
	0.585	4.00				
C	0.585	20.00				
	0.685	0.25				
	0.785	0.25				
	0.825	0.25				
	0.90	0.25				
	1.00	0.25				
	1.10	0.25				
	1.20	0.25				
D	0.585	0.25				
	0.685	0.25				
	0.785	0.25				
	0.825	0.25				
	0.90	0.25				

2.5.2. Phase 2 – Opening Barriers

Multidirectional Wave Basin (MWB)

The Phase 2 experimental protocol was repeated three times for the same openings, but with different temporary barriers. Similar to Phase 1, the test series were separated so that they could reasonably be completed within an eight-hour workday. Leakage rates were measured continuously over 15 minutes intervals.

Table 6. Phase 2 experimental protocol in the Multidirectional wave basin (MWB).

Test Series	Water Level [m]	Duration [h]	Wave Height [m]	Wave Period [s]	Debris Mass [kg]	Debris Impact Velocity [m/s]
A	0.200	0.25				
	0.285	1.50				
	0.585	22.00				
B	0.285	0.25				
	0.285	0.67	0.05	3.00		
	0.285	0.67	0.10	3.00		
	0.285	1.90				
	0.585	0.25				
	0.585	0.67	0.05	3.00		
	0.585	0.67	0.10	3.00		
	0.585	0.67	0.15	2.50		
	0.585	4.00				
C	0.585	0.10			277	1.00
	0.585	8.75				
	0.800	1.00				

Ice Tank (IT)

The Ice Tank (IT) tests were similar to the Multidirectional wave basin (MWB) tests listed above. The only differences being waves were not generated in the IT and were therefore not considered for the barriers tested in this facility, and also the debris impacts were simulated differently (refer to Section 3.3).

Table 7. Phase 2 experimental protocol in the Ice Tank (IT).

Test Series	Water Level [m]	Duration [h]	Wave Height [m]	Wave Period [s]	Debris Mass [kg]	Drop Height [m]
A	0.20	0.25				
	0.285	1.50				
	0.585	22.00				
B	0.0	-			50	0.285
	0.585	0.10				
	0.585	1.00				
	0.80	1.00				
C	0.585	0.25				
	0.285	0.25				

3. Analysis

The following section outlines the various analysis methods used in the estimation of key parameters from the raw data collected during the experiments. The primary parameters were the estimation of the leakage rates (m^3/m/h) through the structure. In general, from the raw data series, it is not possible to differentiate between the leakage, seepage, and overtopping rates (see Figure 4). However, in some cases where the barrier had limited leakage, overtopping estimates became clearer due to the pulse-like nature of the flow rate measurements in the catch basin.

Figure 24 shows the main parameters utilized for the subsequent analysis. The water depth (h, m) is the mean water depth in the basin relative to the floor of the concrete platform (or the base of the superstructure). The relative freeboard (R, m) is the mean water depth above the sill of the opening. For both the water depth and relative freeboard, WP07 was used for the reference measurement. For Phase 1 experiments, the relative freeboard was 0.285 m for the door, 0 m for the basement, and 0.285 m for the east wall. In Phase 2, the sill was 0.15 m above the concrete platform for all of the opening in the Multidirectonal Wave Basin (MWB). For the Ice Tank (IT), the sill was 0.075 m above the platform and the zero was set to 0.075 m below the platform to obtain equivalent water depths as obtained in the MWB relative to the openings.

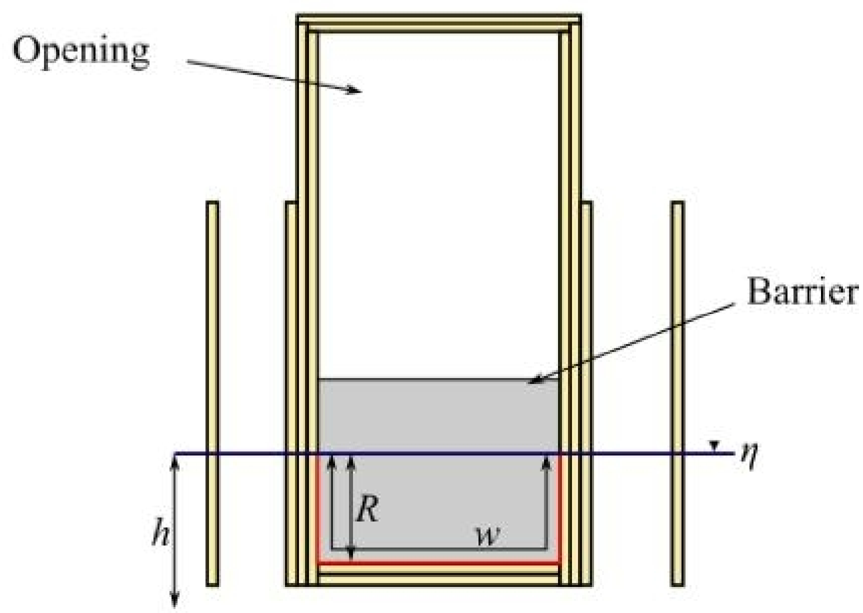

Figure 24. Important parameters for the analysis of leakage rate through the temporary barriers.

The characteristic length of the openings was defined as the wetted perimeter (w - the perimeter of the opening exposed to water). In Phase 1, the basement length was assumed to be the entire horizontal perimeter of the superstructure (21.37 m). The lengths of the north and east wall were assumed to be the length of the catch basin: 4.51 m and 4.41 m, respectively. In Phase 2, the characteristic length was defined as the width of the opening plus twice the water depth. The water surface elevation (η - centered around the mean water depth) was used for estimating the wave characteristics in the basin.

3.1. Leakage Rates

As mentioned above, throughout the experiments, it was not possible to differentiate between leakage around the seal and/or through the barrier, flows overtopping the barrier, and seepage going under the barrier. Since the concrete pad base for the tests was impermeable, seepage underneath the barrier was not an issue. For the majority of cases, water going around the seal of the barrier was the main source of leakage, except in some specific wave condition cases (combinations of waves and water levels) where overtopping was present. The analysis of the data for two different cases was outlined: overtopping (section 3.1.1) and one with one with only leakage (section 3.1.2).

3.1.1. Leakage from Wave Overtopping a Barrier

Figure 25 shows an image with a wave impacting the structure and water overtopping the barrier. The same test is used as an example of leakage rate data where wave overtopping was one of the more influential leakage mechanisms. The test was part of Phase 2 and test series E (TSE) with a Flow Stop regular cushion covering the bottom of a door opening and the leakage data is shown in Figure 26. In cases where the smaller tank was not full before the experiment, the volume flow rate is first measured from the small tank (Figure 26a). The measured water depth is combined with the cross-section of the small tank to calculate the volume. Once the small tank is full and overtops into the weight tank, the volume flow rate is then calculated from the weight tank (Figure 26b). The mass (M, kg) in the weight tank is converted to a volume (V, m^3) assuming a density (ρ) of water of 1000 kg/m^3, it is then combined with the data from Figure 26a resulting in Figure 26c:

$$V = M/\rho \tag{1}$$

The leakage rate is then calculated using the volume change in each tank over each respective interval (Figure 26d). For the majority of cases, the leakage rates were sufficiently different that the values were either taken from the small or large tank. In the case shown in Figure 26, the coarse measurement was sufficient to measure the volume flow rate.

Figure 25. Image from Phase 2: TSE – west door, waves overtopping the FlowStop regular cushion.

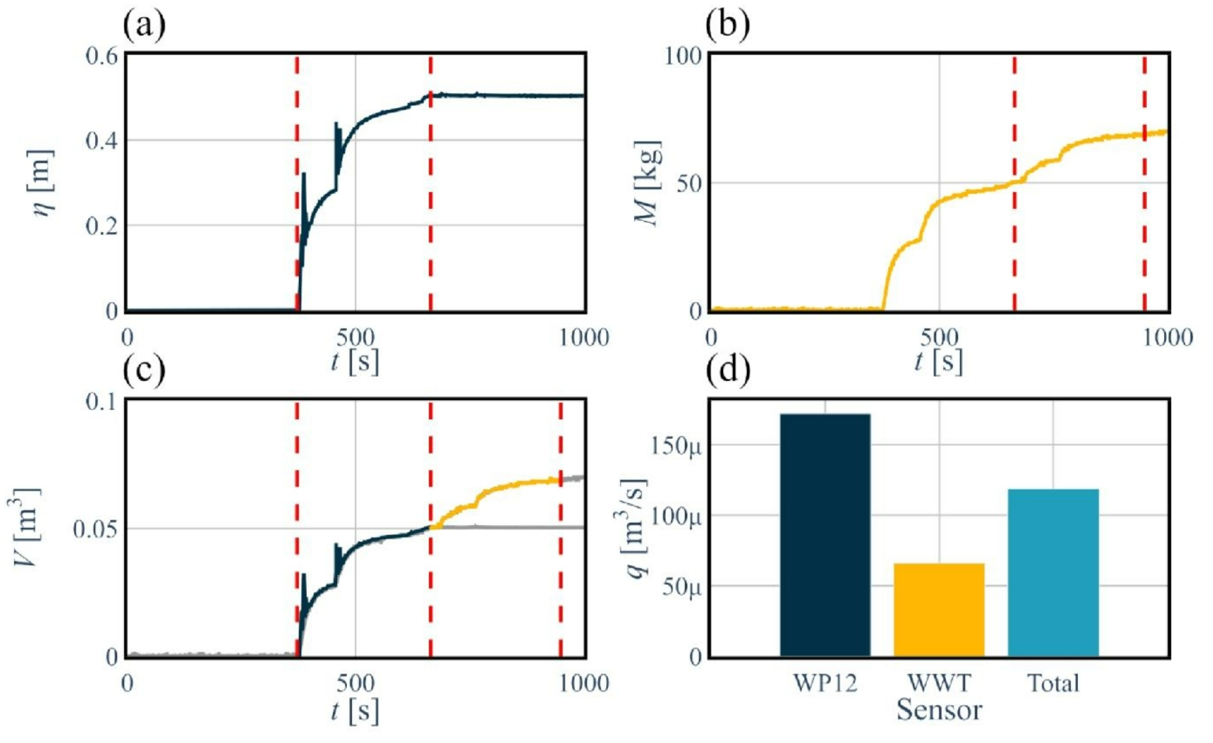

Figure 26. Measurement of overtopping rates. Example taken from Phase 2: TSE – Flow stop regular cushion on the west door opening. (a) water level measurements (WP12) in small tank; (b) weight tank measurements (WWT); (c) combined volume measurements from the two measurement methods; and (d) average overtopping rates measurements from two methods.

3.1.2. Leakage Through or Around the Seal of a Barrier

Figure 27 shows data of the case where the leakage was going through or around the seal of a barrier - taken from Phase 2 Test Series E (TSE) with a plywood board covering a window opening. A photograph of the experiment is shown in Figure 28. A constant flow of water was leaking around the plywood barrier seal and was collected for measurement. In Figure 27a, it can be observed that the water level was consistent throughout the experiment within the small tank being measured by the water level gauge (WP13). This shows that it was already full and was overflowing into the east weight tank. Before the experiment started, water was pumped from the weight tank to reduce the chance of the tank overflowing during the experiments (Figure 27b). The portion where the pump was running was removed from the time series and not considered in the analysis (before first red line). The mass (M, kg) in the weight tank is converted to a volume in Figure 27c. The leakage rate is then calculated using the volume change in the weight tank over the length of the experiment (Figure 27d).

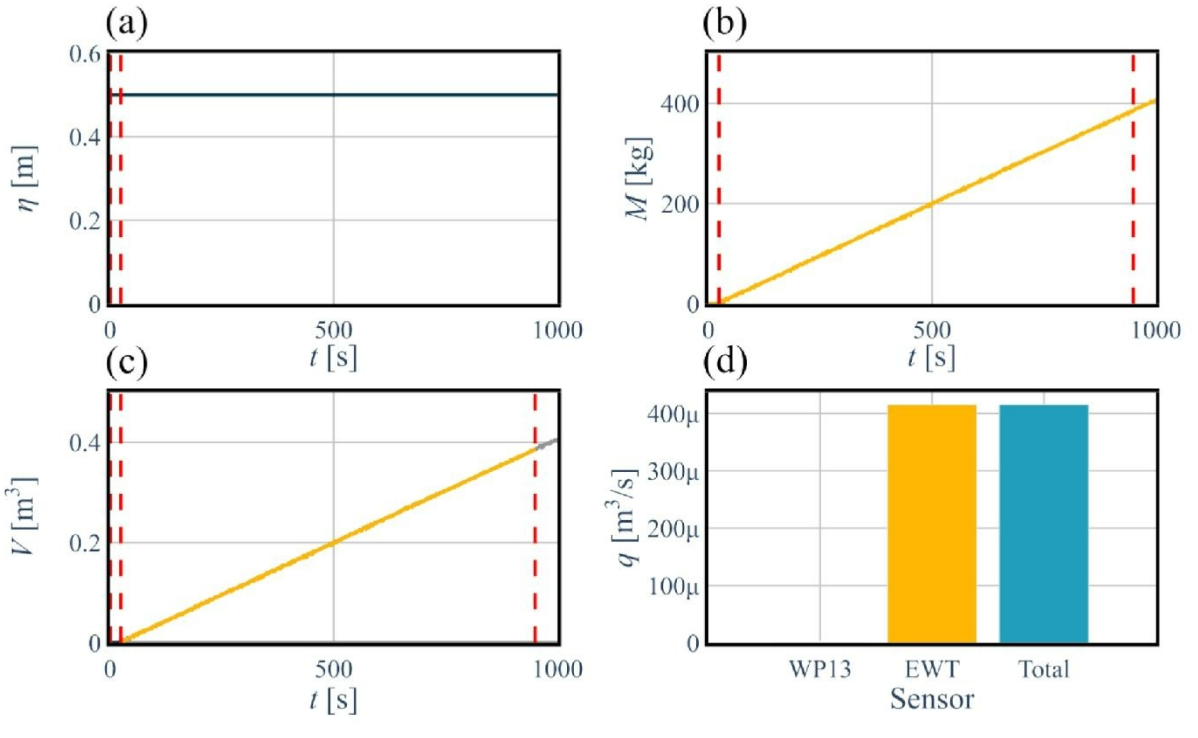

Figure 27. Leakage rates calculation taken from Phase 2: TSE – plywood board over east window opening. (a) water level measurements (WP13) in small tank; (b) weight tank measurements (EWT); (c) combined volume measurements from the two measurement methods; and (d) leakage rates measurements from two methods.

Figure 28. An image of performance testing of flood protection measures, from left to right sandbags, FlowStop full-sized cushion and plywood.

3.2. Wave Analysis

The wave analysis was performed using a frequency domain analysis. The wave time series (Figure 29a) is assumed to be a linear superposition of sinusoids:

$$\eta(t) = \sum a_i \sin(\omega_i t + \varphi_i) \tag{2}$$

where a_i is the amplitude of the sinusoid (m), $\omega_i = 2\pi f_i$ is the angular frequency (Hz), t is the time (s), and φ_i is the phase shift. The spectral density can be calculated from the amplitude:

$$S(f) = \frac{a^2}{2\Delta f} \tag{3}$$

where Δf is the frequency resolution (Hz). Figure 29a shows the spectral energy density of one of the wave experiments.

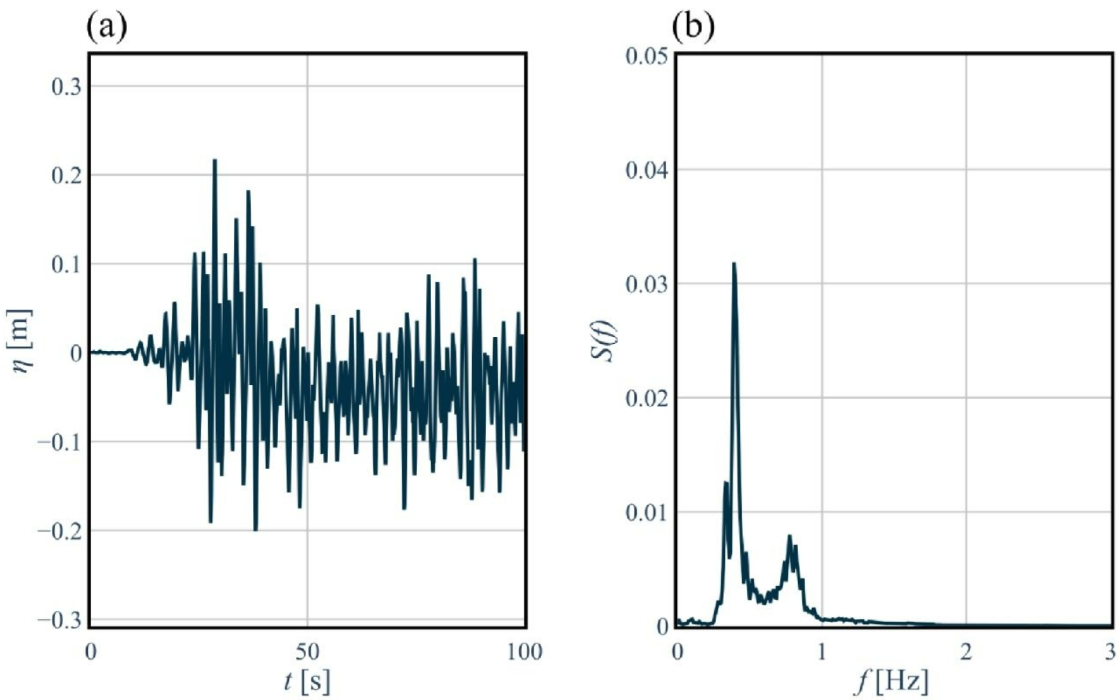

Figure 29. Frequency analysis of wave time series (WP01). (a) Time series of water surface elevation; (b) frequency analysis of water surface elevation.

The characteristic wave height (H_{m0}) can be calculated from the first moment of the spectrum:

$$H_{m0} = 4 \int S(f)\, df \tag{4}$$

The characteristic wave height and peak wave period are often used to represent the wave conditions. The characteristic wave height is approximately equal to the mean of the highest one-third of waves and the peak wave period is the period that is associated with the highest energy waves, or the peak of the wave spectrum such as the example shown in Figure 29b.

3.3. Debris Impacts

There are two types of simulated debris impacts used in the experiments – a different one was used in the MWB and the IT. In both cases the impact energy was 140 J. This is less than the 600 J for the debris impacts recommended by ANSI 2510. The reduced energy was obtained by using the same impactor proposed by ANSI 2510 but using the maximum currents of 1.0 m/s recommended by BSI (2019) as opposed to the 2.0 m/s recommended in ANSI 2510. In the MWB a 277 kg log was saturated by being submerged in water for at least two days and was pulled to achieve an impact velocity of 1.0 m/s. The MWB debris was placed approximately 10 m from the opening barrier and pulled by a motor controlled winch to strike the structure / barrier. The MWB debris was connected to guide wires pulled through pulleys connected to the superstructure at each side of the opening and set to strike at 70º to the opening (20° less than a perpendicular impact). This is shown in Figure 30. The MWB debris was pulled by the winch at a constant velocity that was calibrated beforehand.

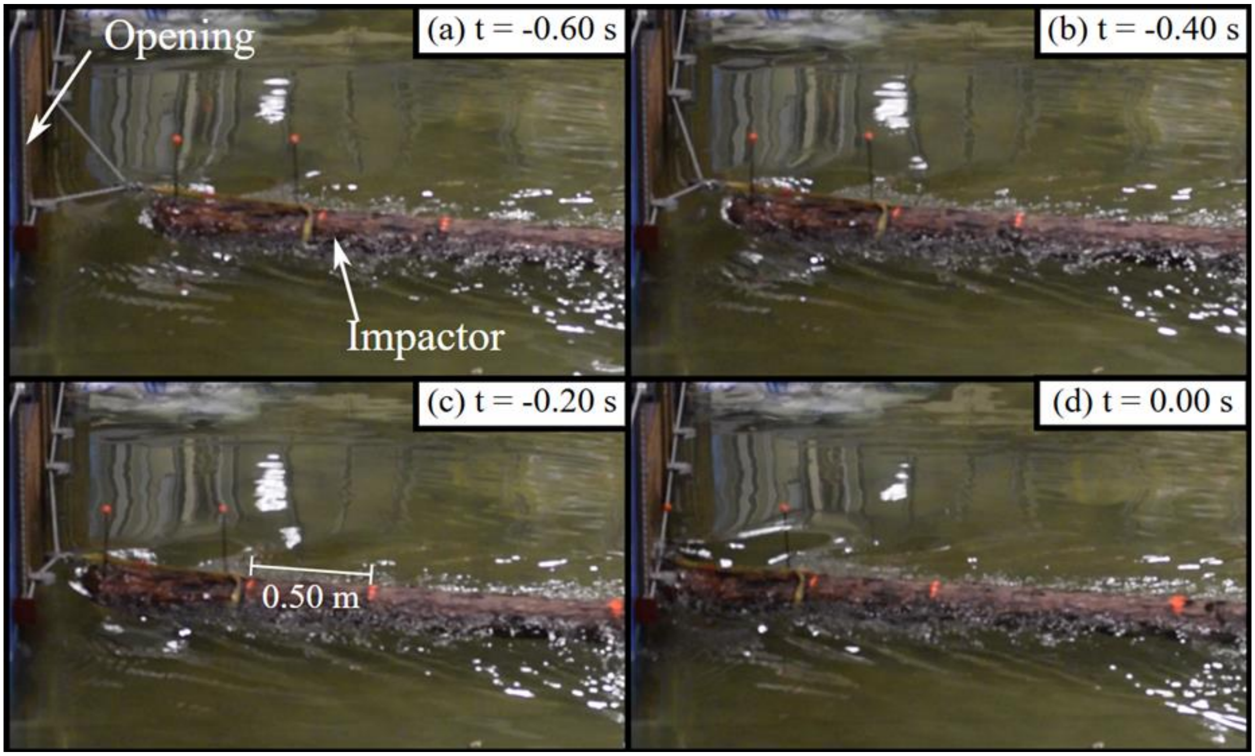

Figure 30. Debris impact testing in Phase 2 in the MWB showing the approach of the debris to a plywood barrier protecting a window opening. The time is provided in reference to the impact time.

The debris impact velocity was measured using a camera (Nikon D5300, 1080 x 1920 pixels resolution, 50 frames per second) placed at the side of the MWB. The debris velocity was measured using the Physlets Tracker Online software (https://physlets.org/tracker/trackerJS/). The images were calibrated using a known distance on the log to calibrate the size of each pixel (Figure 30c). The velocity was measured using the final 5 – 10 images before the log impacted the structure. The accuracy of the debris velocity was estimated to be approximately +/- 0.08 m/s based on repeated analysis of the same test.

To simulate debris impacts in the Ice Tank (IT), a swinging pendulum impactor device was designed and erected in the basin. The impact end of the pendulum was a section of log cut at a 15º angle and attached to a weight so that the total swinging mass was 50 kg (see Figure 31). The IT impactor was suspended by a chain that was 1.25 m long and the centre of mass was raised 0.285 m in elevation from the impact point, resulting in the same 140 J of energy used in the MWB debris impact tests. IT impactor tests were performed in the dry the tank was subsequently flooded (on the same side as the impact) and the same post-impact flood performance tests were completed as in the MWB.

Figure 31. Debris impact testing in Phase 2 in the Ice Tank.

4. Results

4.1. Phase 1 – Residential Home

The objective of the Phase 1 experiments was to evaluate the efficacy of current Canadian residential home design standards to infiltration due to flooding, and assess potential weaknesses in the building envelope. The home was exposed to different flood loads by varying the water depth and wave conditions as shown in Table 5. The focus of this phase of the study is on the volumetric flow rate of water that passes through the building envelope. The performance of the house to resist water penetration was assessed by measuring the flow of water through three main mechanisms – flow entering the home below the floor package, flow coming through the door, and flow coming through the walls. The first signs of water penetrating the structure envelope is shown in Figure 32. The first observations of water entering the structured occurred in the joints between pieces of lumber comprising the sill plate, as this was one of the first parts of the building to get wet.

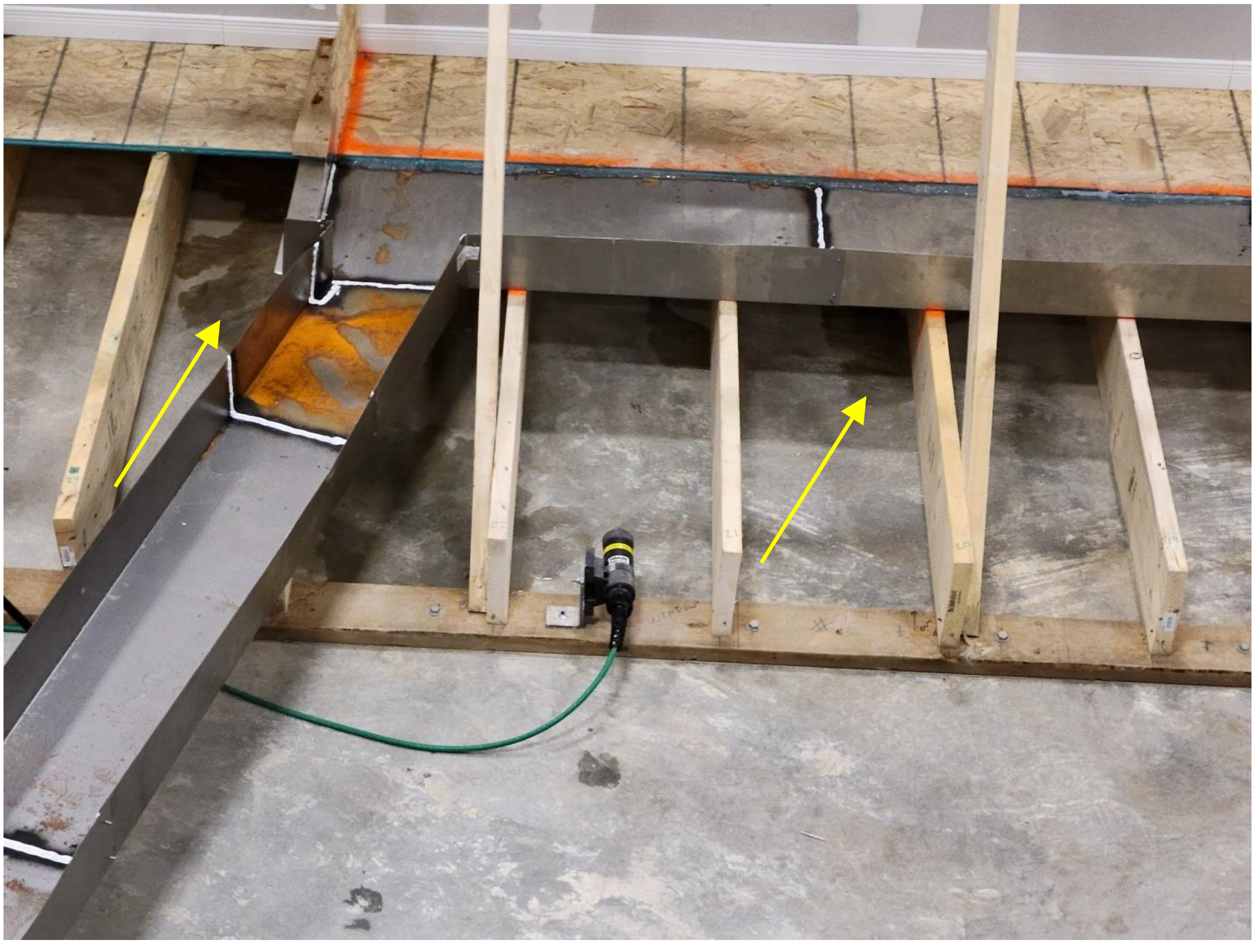

Figure 32. First evidence of leakage observed on top of the concrete pad in Phase 1 testing shortly after exposing the home to rising flood waters.

As the water level was raised above the floor package, water began to leak between the door and the jamb. The leakage was primarily on the latch side of the standard door but as shown in Figure 33, at the deepest water depths (greater than 1 m), there was considerable leakage on the hinge side of the door as well. As shown in Figure 33, the leakage through the standard window during the Phase 1 testing was relatively lower. Leakage can be seen coming through the drywall beneath the window and streaming down the wall, but only a little water entered directly between the window and its frame to form a small puddle on the window sill. This puddle did not reach the edge of the window sill. The leakage observed on the drywall was due to seepage around the window frame installation, presumably due to gaps in the spray foam. This leakage was negligible in comparison with the flow coming through the door.

Figure 33. Leakage through the door observed in Phase 1 at maximum water depth.

The leakage observed through the wall cavity was much lower than what was observed at the sill plate/concrete pad junction and/or coming through the door. As shown in Figure 34, there were on average 2 trickles of water between each floor joist. They are highlighted with yellow arrows. During much of the test period we were incapable of measuring this leakage as it escaped in a small gap between the different sections of the base floor. Once these gaps had been sealed, leakage through the East wall was measured at the end of the Phase 1 tests as shown in Figure 35.

Figure 34. Leakage through the wall cavity in Phase 1. Water trickling off the subfloor identified with yellow arrows.

Figure 35 shows the leakage rate per unit width for the basement, openings, and east wall over the length. The basement measurement is capturing everything below the top of the floor package, from the concrete foundation to 0.285 m in height around the entire 21.37 m perimeter of the structure. The openings measurement is everything above the floor package (0.285 m) within a 4.41 m section of the model home which include the window and the door. . The east wall measurement is everything above the floor package (0.285 m) within a 4.51 m section of the model home. The leakage from the openings was assumed to be principally through the door. No leakage was observed from the window itself, and the infiltration through the wall cavity (as measured from the east wall) was an order of magnitude less than what was observed through the door.

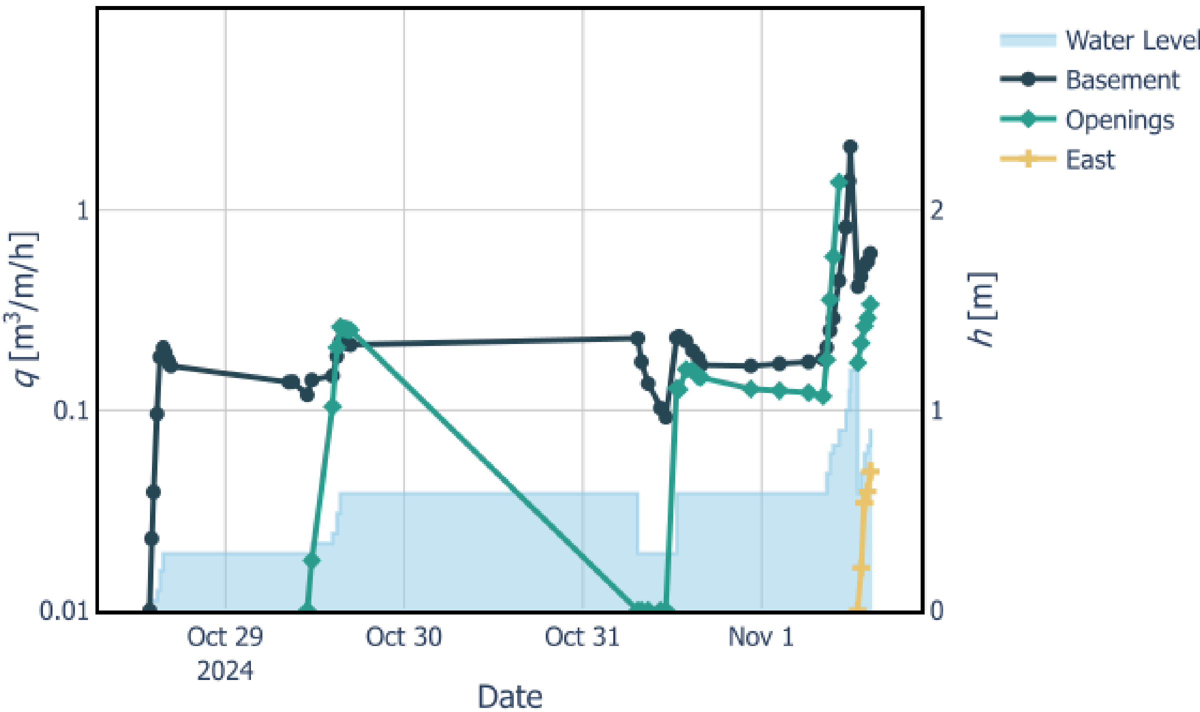

Figure 35. Leakage rate per unit width through the Phase 1 superstructure. The water levels are given in absolute coordinate (referenced to the floor of the raised platform). Time is given in Eastern Standard Time (EST).

The Phase 1 test program did not cause any failure to the building envelope in terms of inelastic structural member failure, visible structural damage to the window or door, or removal of any of the building cladding or drywall. There was significant swelling of the structural members however, but this did not impede the functioning of the window or door at anytime during the test period suggesting that the structural integrity of the model home was maintained. Under the most significant static water loads the door appeared to be deflected open at the bottom corner below the handle. This is evidenced by the large volumes of water entering the structure via this location. However, after the water retreated the door appeared to return to its natural position and sit square within its frame.

Figure 36 to Figure 38 present views of the interior walls and the open wall cavities. The main observable damage was the large amount of water absorbed by the building materials. The first observable damage above the floor package is shown in Figure 36b where discoloration of the dry wall can be observed on each side of the door just above the base boards. In Figure 36c the evolution of the damage is shown as the drywall was wetted above the baseboards further from the door, approximately two stud spacings or 0.80 m on each side of the door. In the same image the drywall is also wet beneath the window indicating that there was water getting into the home through the window opening despite there being no more water visible on the floor below the window than in the other sections of the wall. Any additional water penetration through the window opening appeared to be primarily captured within the wall cavity. No water was visibly entering through the seals of the moving parts of the window and reaching the floor. The most likely point of water ingress was between the window frame and the rough opening.

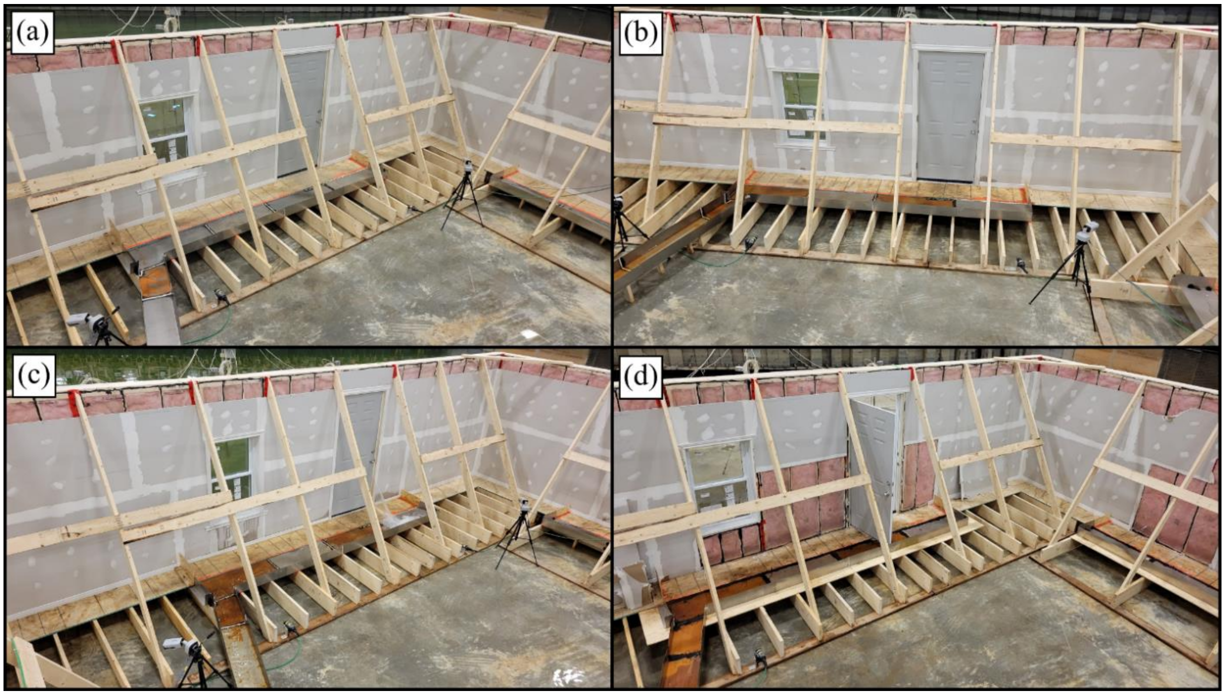

Figure 36. Evolution of water damage to Phase 1 superstructure. (a) Before the start of testing; (b) after the TSA; (c) during TSD; (d) during the deconstruction process. Note – the drywall was removed as part of the deconstruction, not by the flood waters.

Quantifying the water trapped within the structure was out of scope of this study but is evidently very important in assessing flood damage. During the deconstruction period it was noted that water ingress into the wall cavity appears to have primarily occurred between the rim joist and the plywood sheathing as shown in Figure 37. The bottom of the fiberglass insulation was saturated and compressed by the water during the deconstruction of the model as shown in Figure 38. Slumping was not observed in the insulation except under the window where the water saturated insulation represented a much greater fraction of the section of insulation as shown in Figure 36d where the drywall was removed during the deconstruction.

Figure 37. Water damage between the rim joist and the exterior plywood sheathing in Phase 1.

Figure 38. Saturated fiberglass insulation found just beside the door during the deconstruction after Phase 1 testing.

During the deconstruction phase it was noted that the baseboards were completely saturated and broke apart easily when stressed. The drywall remained generally dry and intact although it was saturated and weak at the bottom behind and just above the height of the baseboards as well as below the window. The vapour barrier was effective at keeping most of the drywall dry over the test period. Future tests to examine damage to the drywall could include increasing the flood exposure time and slowing the removal of flood water from the dry side of the model.

In general, the leakage rates increased as water levels increased above the opening height (Figure 39). For the opening measurement, most of the observable leakage passed through the door. There was an appreciable increase in leakage as soon as the water level was above the door base. The leakage rate did not increase as much when the water level rose above the base of the window, again showing the door was the main source of leakage. For the east wall, some leaks were observed in the catch basin that were repaired after test series C; so the contribution of this wall to the leakage rates is understated in the data from test series A to C, hence, the limited measurements seen in Figure 39.

As the testing progressed, for a given water level a decrease in the leakage rate was observed which was attributed to the expansion of the wood as it began to saturate (thereby reducing gaps and leakage pathways). Over the duration of the experiments (5 days and 52 hours of flood exposure), the expansion of the wood resulted in a 59% reduction in the leakage rate of the basement for R = 0.285 m and a 29% reduction in the leakage rate of the basement for R = 0.585 m. The openings had a reduction in the leakage rate over the experiments of 54% for R = 0.30 m. It appeared that to a certain extent the increase in water depth counteracted the influence of the wood expansion; however, further tests would be needed to explore this relationship. Moreover, since these tests exposed the home to 52 hours of testing (flood exposure), further testing is recommended to investigate the time dependency of flood exposure to decreasing leakage rate (due to the wood expansion), and whether prolonged exposure results in another mechanism that may increase the leakage rate (like structural failure of membranes, drywall, vapour barrier, etc.).

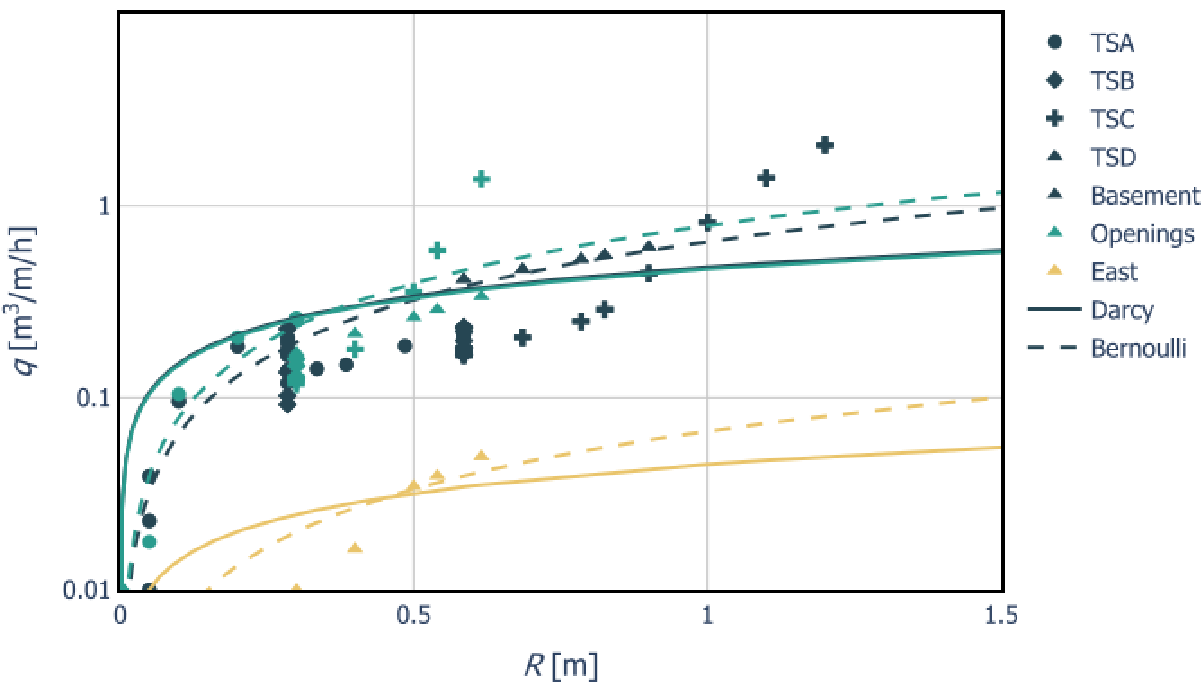

Figure 39. Leakage rate per unit meter versus the relative freeboard through the Phase 1 superstructure. The water level is referenced to the height of the opening: 0.285 m for the opening and east and 0 m for the basement. Lines are the fitted parameters from Table 8.

In general, leakage rates for the same absolute water depth were dominated by the basement leakage. Figure 40 shows the leakage rate for the last test series where the wood is at its highest saturation and expansion level (and the leakage is at it lowest relative level). Leakage rates for the basement were consistently larger than the other sources with values being 1.8 – 2.4 times greater than the openings and 12 – 15 times greater than the leakage contribution from the east wall (Figure 40).

When the leakage rates are corrected for the difference in opening heights and normalized for length (Figure 39), the leakage rates through the openings section (0.285m above the concrete foundation and

4.41 m long) are approximately equal or greater than the basement leakage rates (0.00 m above the foundation and 21.37 m long). This could be partially attributed to the openings not being completely saturated due to less time underwater as there is an appreciable difference between the leakage rates measured for like water depths in test series C, where the structure was flooded for 1 day in advance and test series D where the structure had been dried to execute a repair.

For the openings and the basement, the leakage through the building envelope seems to commence almost immediately when exposed to water. For the east wall, there is a lag in the onset of leakage. The lag may be due to relatively small leakage rates which cannot be measured with the catch basin system for this area. Assuming a static system, two theories from civil engineering can be used to describe the leakage rate. Assuming minimal losses, the rate of leakage through the structure q (m^3/h) would be expected to be approximately proportional to $\sqrt{R}$, where R is a characteristic volume (m^3) (Bernoulli, 1738):

$$q = \sqrt{2gRh_o} \times 3600 \quad (5)$$

where g is the gravitational acceleration (m/s^2) and h_o is the height of the fluid above the opening where the water penetrates (m). As the water can penetrate from a range of sources, the $3600\sqrt{2gh_o}$ term can be combined into a single parameter B (that has the units of $m^{3/2}$/h).

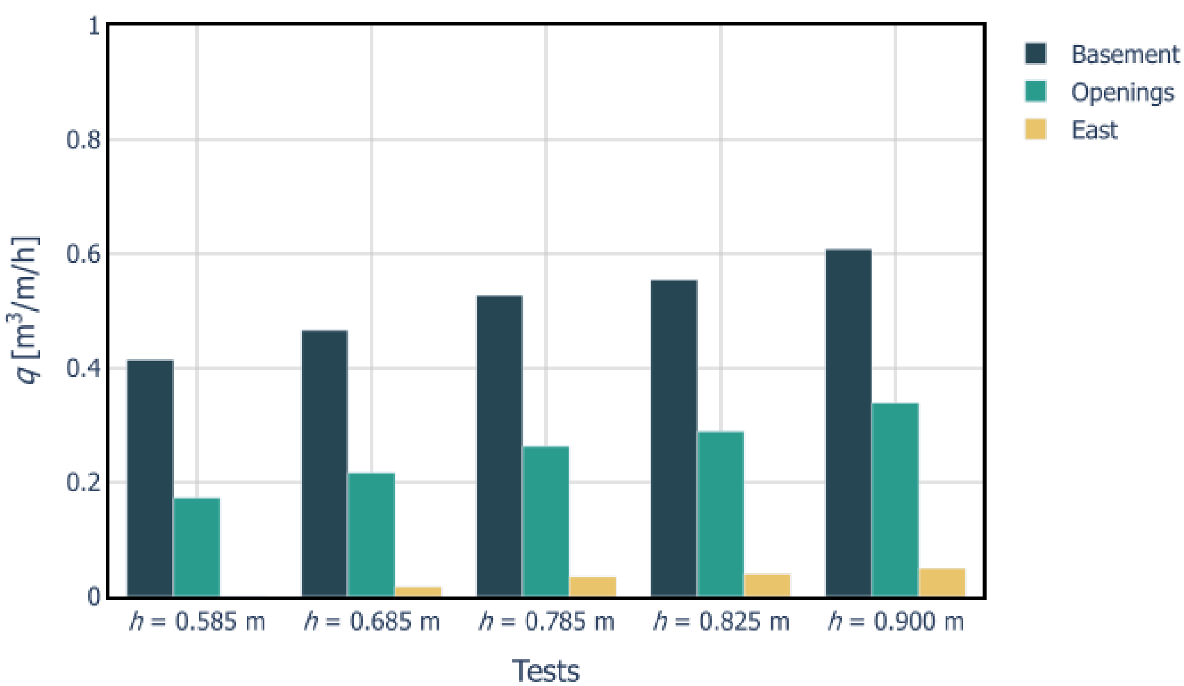

Figure 40. Influence of water depth on leakage rate through Phase 1 structure.

Assuming the openings and walls act like a porous medium, Darcy's law could be applied:

$$q = KR' \tag{6}$$

where K is the hydraulic conductivity of the opening (m/h) and *R'* is a characteristic area (m^2). Eq. (5) and Eq. (6) were fit to the data for each source, the fitted parameters can be found in Table 8 and the corresponding functions can be seen in Figure 39. It was assumed that with zero freeboard, the leakage rate through each source would be zero. In general, the linear relationship (Darcy's Law) fit better to the data collected in this study. However, it should be noted that all the tests were included in the fitting, and as described earlier, the wood saturation level was not constant through all the tests, and its effect on porosity and leakage rate may influence the fit. Furthermore, limited data was collected for the east wall resulting in a strong correlation coefficient that may not be representative of larger data sets.

Table 8. Fitted parameters describing leakage rates through the various sources in Phase 1.

	$\sqrt{\boldsymbol{R}}$ ($m^{3/2}$)		$\boldsymbol{R'}$ (m^2)	
Source	$\boldsymbol{B}$	**Pearson's r**	$\boldsymbol{K}$	**Pearson's r**
Basement	0.479	0.65	0.65	0.74
Openings	0.469	0.59	0.79	0.69
East	0.045	0.98	0.067	0.99

Figure 41 shows the six experiments where waves were included. The influence of the wood expansion can be observed in these tests (which occurred near the mid-point of the experiments) with a gradual decrease in the leakage rate as the test progressed. A slight increase was observed for the openings between waves tests; however, this is difficult to attribute to the change in wave heights. No damage was observed as a result of the waves so the only source of leakage from the waves would be the change in dynamic pressure, which would be symmetric around the mean water depth and at most add approximately 20% to the total pressure (based on linear wave theory) at the opening height. Therefore, for the analysis above, the waves were not considered to be significant.

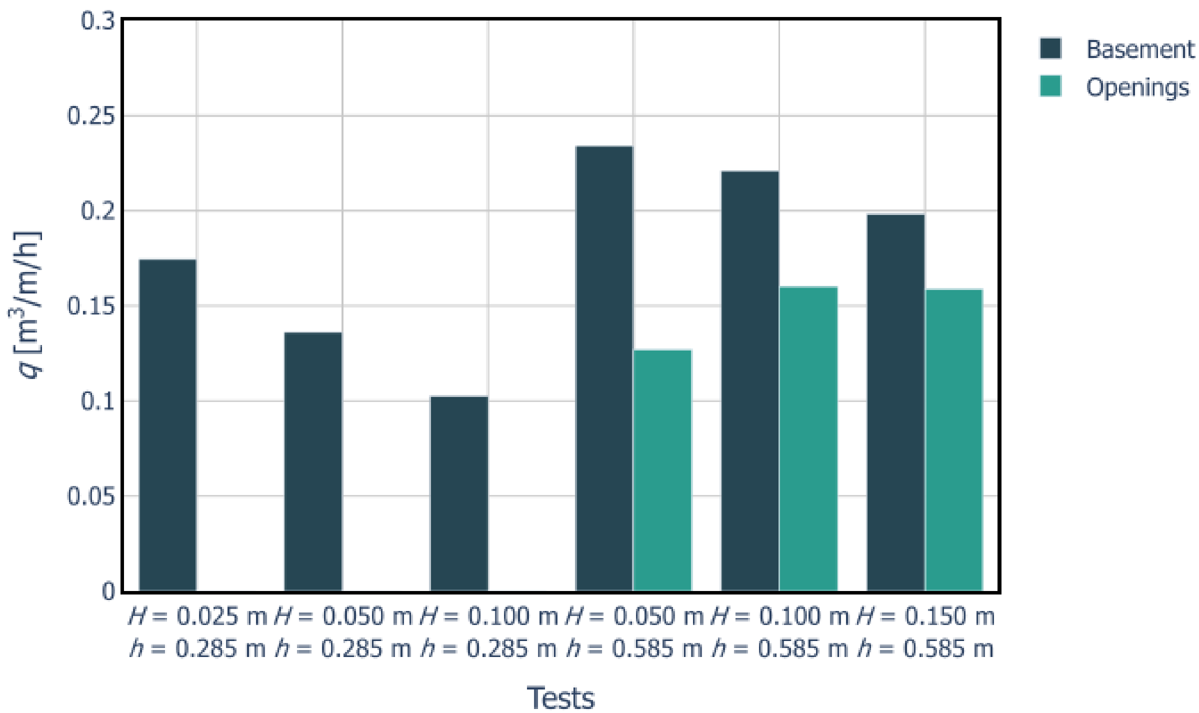

Figure 41. Leakage rates per unit length for Phase 1 superstructure under the influence of various combinations of water depth and zero-moment spectral wave height.

4.2. Phase 2 – Opening Barriers

4.2.1. Opening Barrier Ease of Installation

One of the key criticisms of using sandbags for emergency flood response is the time and resources required to perform the setup (Pinkard et al., 2007). One of the key advantages of proprietary systems is that they are designed to be easily and rapidly mounted and dismounted in the event of an emergency. Therefore, it is critical to assess overall performance against the technical difficulty in implementing the barrier. However, due to the range of facilities and NRC technical staff used in this experiment, it was challenging to have a quantitative assessment for all of the barriers. Therefore, the technical staff was instead surveyed after the experiments on each of the barriers and asked to provide a score from 1 – 5 with one representing a barrier that was easy to install and/or needing a low amount of labour/expertise, and five being hard to install or requiring a higher amount of labour/expertise (Table 9). The technical staff was asked to consider how the barriers would be installed in their homes (i.e. if they were to have only the tools that and average homeowner would possess). Each of the barriers was rated on:

- Time to Setup: the amount of time it took for a person to read the instructions and implement the barrier.

- Technical Expertise Required: how challenging the installation of the barrier was factoring in the complexity of the required tools to perform the installation.
- People Required: how many people would be needed to install the barrier in an efficient manner.
- Ease of Instruction: how easy was it to understand the instruction manual provided with the barrier.

The standard infrastructure barriers (the actual doors and windows) were not evaluated as it is assumed that these barriers would already be in place and would not necessarily be installed by a homeowner during an emergency.

Table 9. Ease of installation of each of the opening barriers. Each category was assessed on a scale of 1 – 5 with a five being the highest.

Opening	Barrier	TIME TO SETUP	TECHNICAL EXPERTISE REQUIRED	PEOPLE REQUIRED	EASE OF INSTRUCTIONS	Average Score
WINDOW	Plywood	1	2	1	1	1.25
	Sandbag	5	2	5	2	3.5
	Sliding Window	N/A	N/A	N/A	N/A	
	Awning Window	N/A	N/A	N/A	N/A	
	Flow Stop Full-Sized Cushion	1	1	1	2	1.25
	Aqualock Window Protector	2	5	2	2	2.75
	RS Stepanek	2	3	1	1	1.75
DOOR	Standard Door	N/A	N/A	N/A	N/A	
	DamEasy	1	2	1	1	1.25
	Flow Stop Full-Sized Cushion	1	1	1	2	1.25
	Flow Stop Regular Cushion	1	1	1	2	1.25
	Stormmeister Flood Resistant Door	5	5	3	5	4.5
	Aqualock Quickwall	3	5	1	4	3.25
	Stormmeister Rapid-Assembly Log-Type Barrier	3	4	2	4	3.25

In general, the barriers that had semi-permanent components (Stormmeister Door and Barrier, Aqualock Window Protector, and RS Stepanek) tended to be among the most difficult to install. The majority of these products did suggest having an experienced contractor do the initial installation to ensure water tightness. The sandbags were most challenging, primarily related to the resources and time and effort required for the setup, and this sentiment aligns with the opinions of Pinkard (2007).The temporary measures, such as the Flow Stop and plywood, were the easiest to install.

4.2.2. Barrier Performance

The main objectives of Phase 2 was to evaluate the performance of various opening barriers in comparison with the leakage rate experienced through the opening infrastructure itself (through a Canadian standard window and door), and also compare the flood barriers performance versus the more commonly used flood protection measures for openings (such as sandbags and plywood covering). All the barriers were also compared to the acceptable leakage rate threshold defined in the ANSI 2510 standard, 0.001 $m^3/m/h$ over each 15-minute measurement. The definition of the dimenston of the opening can be found in Section 3. The performance of each of the temporary opening barriers over the experimental protocol is shown in the present section. Figure 42 shows an example of opening flood barrier performance for the entire duration of the testing protocal. The water level throughout the protocol is shown as the faded blue box, the ANSI 2510 threshold of 0.001 $m^3/m/h$ is shown as the dashed black line, and the tests for waves and debris impact are delineated by the dashed grey lines (the tests occurred between the grey lines). Each marker shows the time when the 15-minute increment was started. Breaks in the leakage measurements show data that was lost due to malfunctioning instrumentation or other issues that led to measurement accuracy. Any values less than 0.0001 $m^3/m/h$ were considered to be below the measurement threshold within the multidirectional wave basin and they were not included. If the barrier was significantly damaged or the leakage rate exceeded 20 $m^3/m/h$ (and started to overflow the measurement tanks), the barrier was considered to have failed and a red cross was placed over the last measured value (for example, sandbags in Figure 42).

As shown in Figure 20, the first set of tests in the MWB investigated the performance of a plywood board and a sandbag barrier on window openings (these two comprising the most commonly used “reference” opening barriers), and a FlowStop full-sized cushion and a 0.90 m high FlowStop regular sized cushion on door openings. Figure 42 shows the performance of these barriers through the testing protocol. Throughout the tests, the sandbags and plywood showed leakage rates significantly above the ANSI 2510 threshold. The leakage through the sandbags occurred primarily through the contact points between the sandbags and the bed or the connection seam between the sandbags and superstructure walls. The high volume of leakage bypassing the sandbags rapidly overcame the measurement tanks which impeded further results early in the experimental protocol. A piece of plywood was placed in front of the opening and held in place with the sandbags to prevent water from overwhelming the dry pit. Previous research (Massolle et al., 2018) noted that sandbag performance was highly dependent on the surface where they are placed, so the leakage rates presented in this study (on a concrete bed) may not be representative of all bed conditions. In the Massolle et al. (2018) study, leakage rates for sandbags on a natural turf surface were an order of magnitude (approximately 1 $m^3/m/h$) smaller than those observed in these NRC experiments. It should be noted that the in the present study the seal length is defined as the wetted perimeter of the window opening exposed to flooding (*w* from Figure 24) and not the contact length of the sandbags as used by Massolle et al. (2018). This increased the leakage rates in this work by a factor of 2.8 when comparing to the Massolle study. Further, in the present experiment, a sandbag wall 2-3 bags wide was constructed in the limited space around a window. In Massolle et al. (2018), a much larger pyramid structure was constructed resulting in a thicker wall, additional “contact length”, and less water infiltration. In summary, the Massolle study better reflects the typical use of a sandbag wall to surround an entire house, while the present work is highlighted the specific case of protecting only an opening such as a window or door. In both cases the sandbag wall could be improved by weaving a polyethylene layer between the sandbags such as discussed in Massolle et al. (2018). This benefit would be reduced in the case of protecting an opening where the perimeter of the sandbag wall, both footprint and wall contact, is high in comparison to the protected area (opening width x water depth).

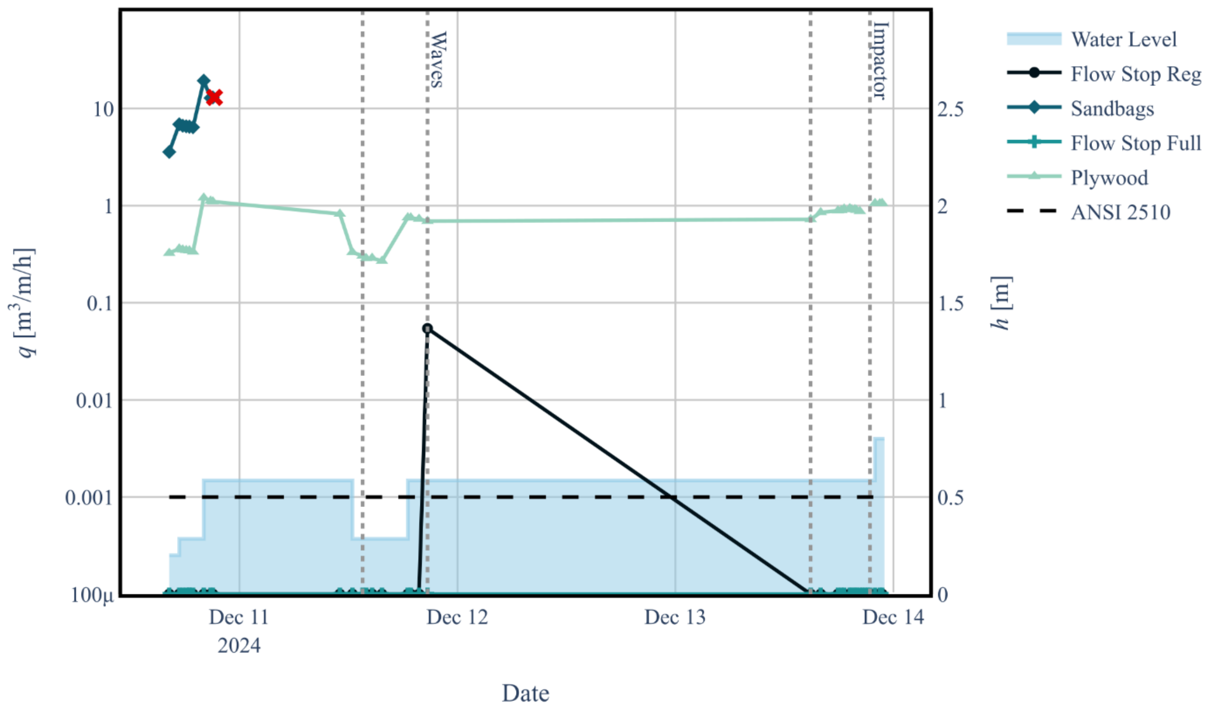

Figure 42. Leakage rate per width of the opening for first run through the experimental protocol in the MWB.

The rate of leakage through the plywood opening barrier varied directly and fairly linearly with the depth of the flood (i.e. as the water depth increased the leakage increased). The two Flow Stop barriers had negligible leakage rate for the majority of the protocol, except for the combinations of the largest wave height with deeper water depths for the Flow Stop regular cushion. This barrier only covered the bottom portion of the door (0.90 m) and the main leakage mechanisms was due to wave overtopping the top of the barrier as shown in Figure 25.

Figure 21 shows the protective measures used for the second set of tests in the MWB. The performance of a RS Stepanek on a window opening, a standard door, a standard sliding window, and a DamEasy barrier on a door opening were all tested. Figure 43 shows the leakage results runoff these barriers through the experimental protocol. The RS Stepanek barrier performed well throughout the testing with minimal leakage. A small amount was measured early in the test series (well below the ANSI 2510 threshold), however, the barrier seemed to adjust and no significant leakage was observed for the rest of the protocol. It is possible that this recorded leakage was in fact condensation. The barrier is metallic and the water in the basin was very cold. There was considerable condensation on the interior surface of the barrier. The seals also appeared wet so the source was not clear but the volume was very small. It is important to note the sliding window used here in Phase 2 (vertical seam between the two window panes, slides side to side) is different than the window used in Phase 1 (horizontal seam between the window panes, slides up and down). This Phase 2 sliding window showed significant leakage rates, much higher than the window used in Phase 1, and the flow came primarily between the two window sections as shown in Figure 44. For the standard door, the leakage came primarily between the door and the frame as we observed in Phase 1. The DamEasy showed leakage rates above the ANSI 2510 threshold, and it failed suddenly during the wave experiments completely detaching from the opening as shown in Figure 45. The DamEasy (0.76 m) barrier is lower than the Flow Stop regular sized cushion (0.90 m) so the overtopping was also greater than what was discussed in section 3.1.1. During the wave tests, the DamEasy was observed to have observable deflection under wave action. A small increase in leakage rate was observed throughout the wave tests so an effect of cumulative displacement could have contributed to the failure of the DamEasy. In Figure 45a we see that the wave which caused the failure was quite large splashing at the top of the impermeable structure, more than 1 m above the mean water level.

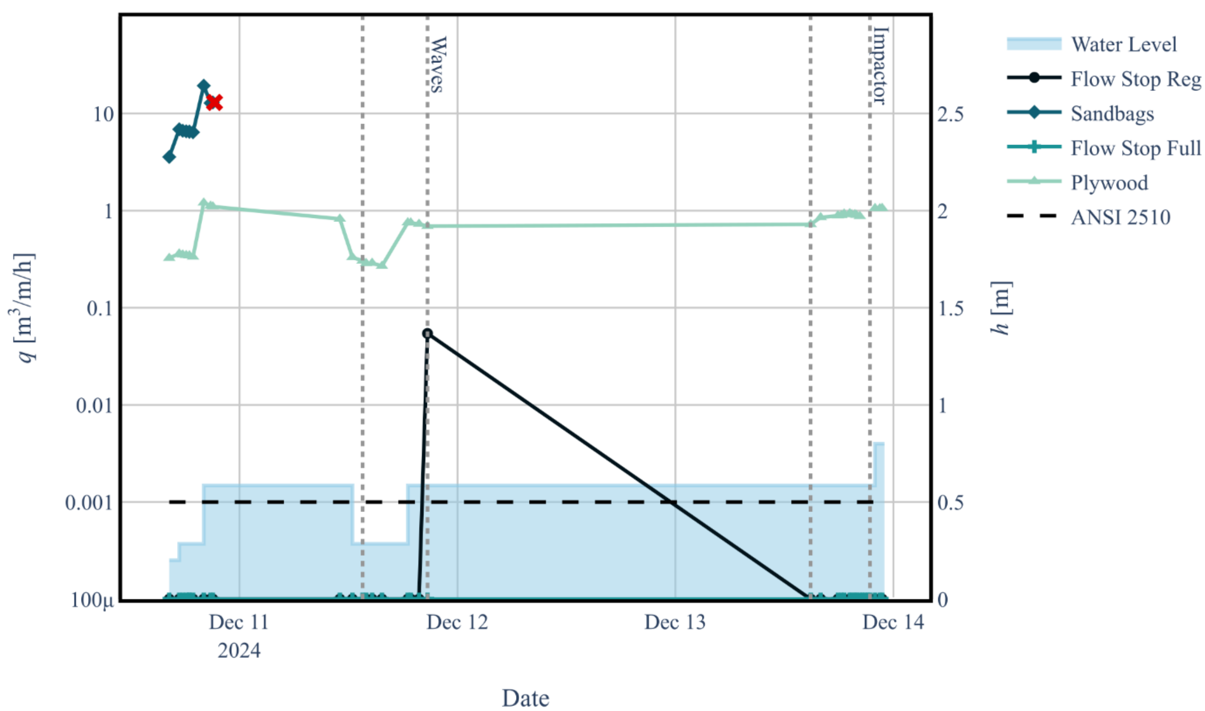

Figure 43. Leakage rate per width of the opening for second test series in the MWB.

Figure 44. Leakage observed between the two panes of the sliding window in the MWB.

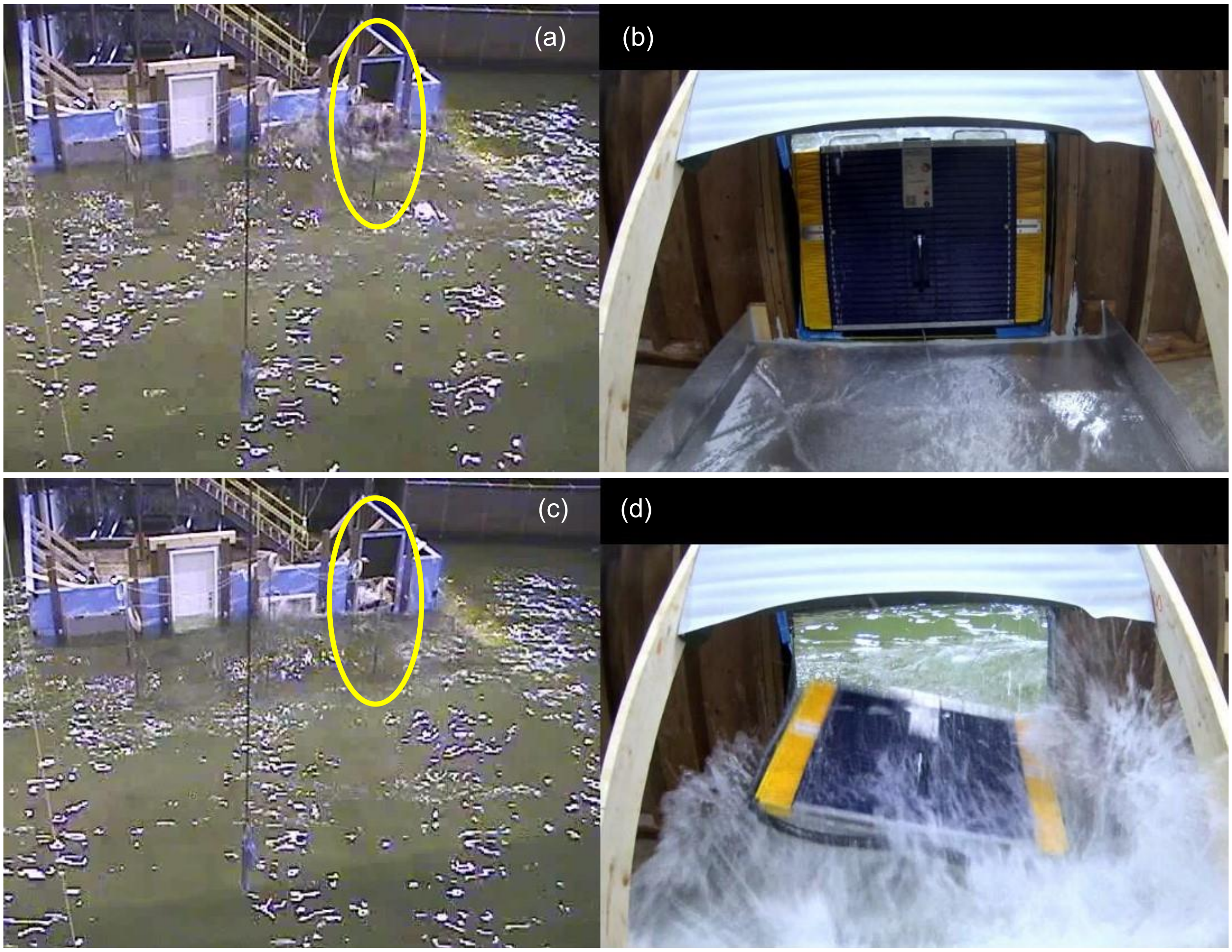

Figure 45. Failure of the DamEasy barrier under wave action. (a) shows the wave crashing against the structure, (b) shows the barrier as the wave crashes, (c) and (d) show the barrier at the moment of failure.

As shown in Figure 22, the third set of tests in the MWB investigated the performance of an awning window; a standard door in conjunction with a DamEasy barrier, a sliding window used in conjunction with a plywood board, and a Stormmeister flood resistant door, and Figure 46 shows the results through the testing protocol. In this run, water penetration through all of the barriers exceeded the ANSI 2510 threshold. The Stormmeister flood resistant door failed during the impact testing as shown in Figure 47 and Figure 48 – and it is important to note the impact energy used (140 J) was well below that specified in ANSI 2510 (600 J). Before the failure, the leakage occurred mainly through the seal under the door. In Figure 48, in the lower right image, two glazing beads are projected towards the camera during the failure and water is seen leaking through the central panel. A plywood panel was inserted over the Stormeister door within seconds of the failure. The Stormmeister door was not completely dislodged from the impact test failure, but was compromised in terms of its ability to resist the flood water. For the standard door used with the DamEasy and also the sliding window used with the plywood barrier, the intention was to evaluate the effect of a barrier system versus the performance of the individual units. For both systems, the combined barriers showed similar performance to the individual best performing component. In the case of the sliding window with plywood, there was also a migration of the primary leakage to around the frame of the window (similar to the leakage through the plywood). The awning window leaked primarily through the seal between the window and the window frame.

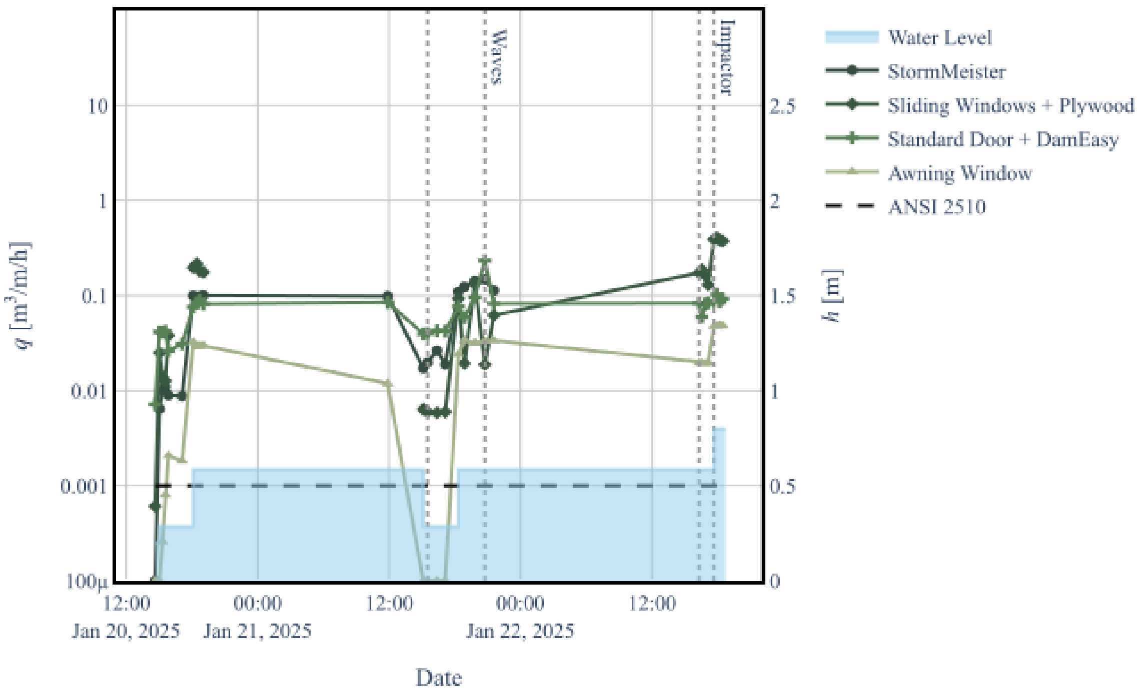

Figure 46. Leakage rate per opening width for the third test series in the MWB.

Figure 47. Debris impacting the StormMeister door just prior to failure.

Figure 48. Failure of the StormMeister door under debris impact.

As shown in Figure 23, the set of tests in the IT investigated the performance of a Flow Stop full-sized cushion and an Aqualock Window Protector in window openings and a Stormmeister Rapid Assembly Log type Barrier and an Aqualock Quickwall in door openings, and Figure 50 shows the results from experimental testing protocol. The set of experiments in the IT were only run for one series. The leakage through the Flow Stop full-sized cushion and the log type barrier were higher than the ANSI 2510 threshold of 0.001 m^3/m/h. The leakage through the AquaLock Window Protector was primarily through the edges of the wood where the barrier was attached as per the manufacturer's recommendation. A lumber frame was fastened to the tank as per the manufacturer recommendations using mechanical fasteners and silicone to seal to the blue skin. The Aqualock was sealed to the wood frame using an adhesive product provided by the manufacturer. Under flooding conditions the water appeared to saturate the wood and a constant trickle of water was evident. It was technically challenging to adhere a heavy and flat material to a vertical structure without mechanical fasteners, and ensure a water tight seal. This challenge was raised with the supplier prior to installation and they provided some advice, but there was a very small amount of leakage here that could be reduced or eliminated with mechanical fasteners applying additional pressure to the seal. The leakage on the Aqualock Quickwall and the log type barrier were occurring from the lower seals. In both cases there is a frame adhered along each side and the bottom of the doorway. In the event of a flood a wall is quickly built sealing against this frame. These seals are made of rubber or neoprene respectively. There was nothing visually wrong with either seal. After the impactor tests both walls were inspected for debris or damage along the frames and seals. No issues were found. The seals were wiped however, there was no improvement.

The ASNI threshold of 1.0 l/m/h is a very small amount of water. The AquaLock window protector is shown in Figure 49 during the most severe leakage conditions, Test Series N at a water level of 0.585 m or 0.335 m above the window threshold. Under these conditions the leakage rate reached a maximum of 0.0039 m^3/m/h. This is almost four times the ANSI 2510 threshold. At this rate the leakage is approximately 2 ml each second. At this point it was a constant dribble. The log type barriers reached a maximum of 0.0008 m^3/m/h. More advanced log type barrier systems provide a combination of mechanical fasteners and adhesives for the C-channels and an installation which provides a more consistent application of pressure on the gaskets which should improve performance by providing both a more secure and more water tight seal. The threshold for the ANSI standard is stringent likely because even a little water inside a home can cause a great deal of damage. It can also be technically challenging to reliably collect such small volumes or provide seals of that quality. The quality and durability of seals can be especially challenging for products that with installed frames which may spend years exposed to the elements before they are put to use.

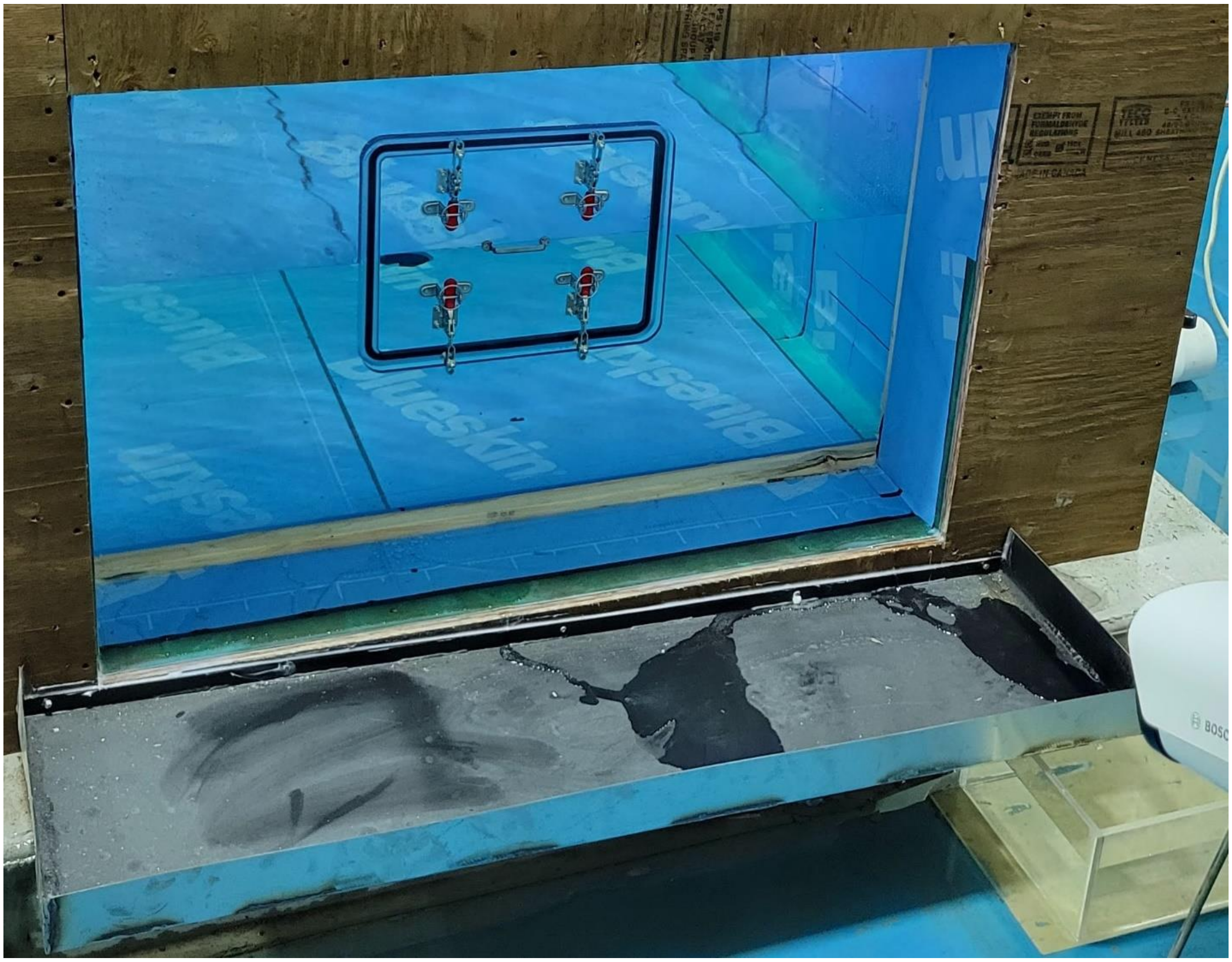

Figure 49. Leakage from the AquaLock window protector, Test Series N and a water level of 0.585 m.

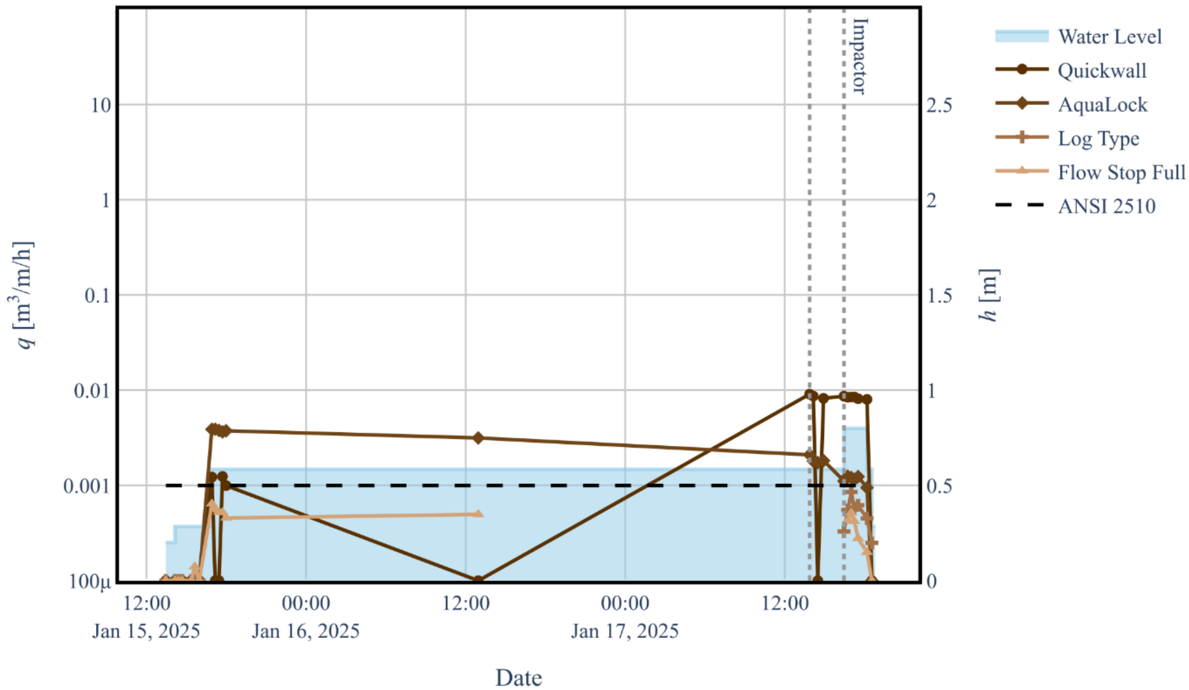

Figure 50. Leakage rate per unit width of the opening for the IT experiments.

Figure 51 shows the performance of each of the opening barriers for the corresponding freeboard (water depth above the sill of the opening) for the data acquired in Phase 2. Consistently, the leakage rate of the barriers increased with increasing freeboard. Despite being the most commonly used barriers historically, the sandbags and the plywood “reference” barriers tended to be the poorest performing. The standard pieces of infrastructure that are used in the openings, i.e. the standard door and sliding window also performed poorly. In general, the majority of barriers did not achieve the ANSI 2510 leakage rate threshold, despite the majority of them having previously passed the standard through FM Approvals. The cause of this difference in results from the ANSI standard to the tests performed here could be from a variety of sources, and it should be noted that NRC was not privy to the installation or testing conditions from the ANSI 2510 tests. The Phase 2 testing prototcol performed herein used an opening of wood covered with the Blueskin membrane. This membrane may be smoother than what would be typically found in an opening. The testing for ANSI opening barriers often is performed with the developer of the technology present to provide guidance on the installation and operation of their barrier. For these tests, the barriers were installed by the NRC technical staff according to the provided specifications. Differences in the familiarity with the product may have influenced the results. However, such discrepancies in the performance due to installation sensitivities are important to document as in most cases these barriers will be installed by the inexperienced home-owner, and not experienced professionals with specialized tools. This is specifically a concern for the barriers which had incorrect or incomplete instructions. Finally, due to challenges in the setup and duration of the testing, only one test run protocol per barrier could be performed so it is difficult to assess repeatability analysis on the data, or complete sensitivity analysis due to differences in installation. Common traits of success for the barriers were a large contact area for the seal, 4.5 cm or greater, and the use of mechanical fasteners where adhesives or sealing compounds are used.

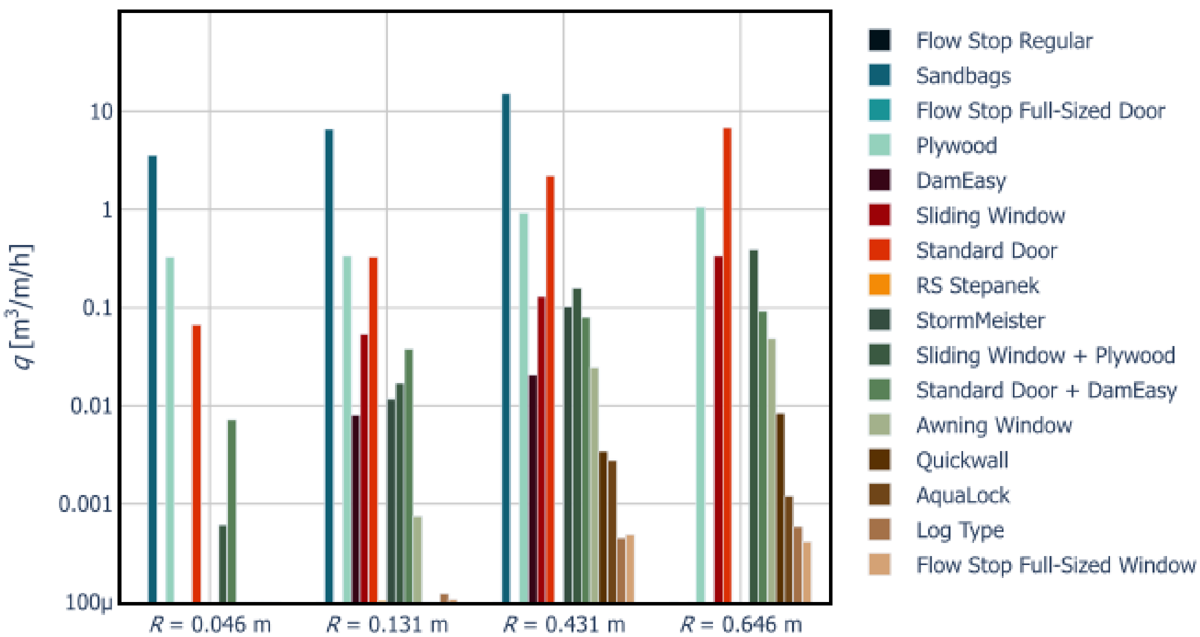

Figure 51. Average leakage rate per unit width as a function of freeboard for each of the barriers tested in Phase 2. The figure combines the tests from the MWB and IT.

Figure 52 shows the influence of the wave tests on the opening barrier performance. Unlike the Phase 1 testing, there does appear to be an observable difference in the barrier performance due to incident wave height (increasing wave heights show increased leakage rates). However, it is clear that the performance of the barrier is influenced more by the freeboard as opposed to wave conditions. The wave conditions became increasingly important when overtopping could occur (as in the case of the DamEasy and Flow Stop regular cushion which only cover the lower portion of a door opening). However, this was only observed for the highest wave height. Deflection due to the hydrostatic forces or the dynamic forces from the waves/debris impacts was not measured in this study. However, in the case of the Flow Stop full-sized cushion significant displacement occurred, and the DamEasy barrier deflected substantially and then failed by coming dislodged from the opening.

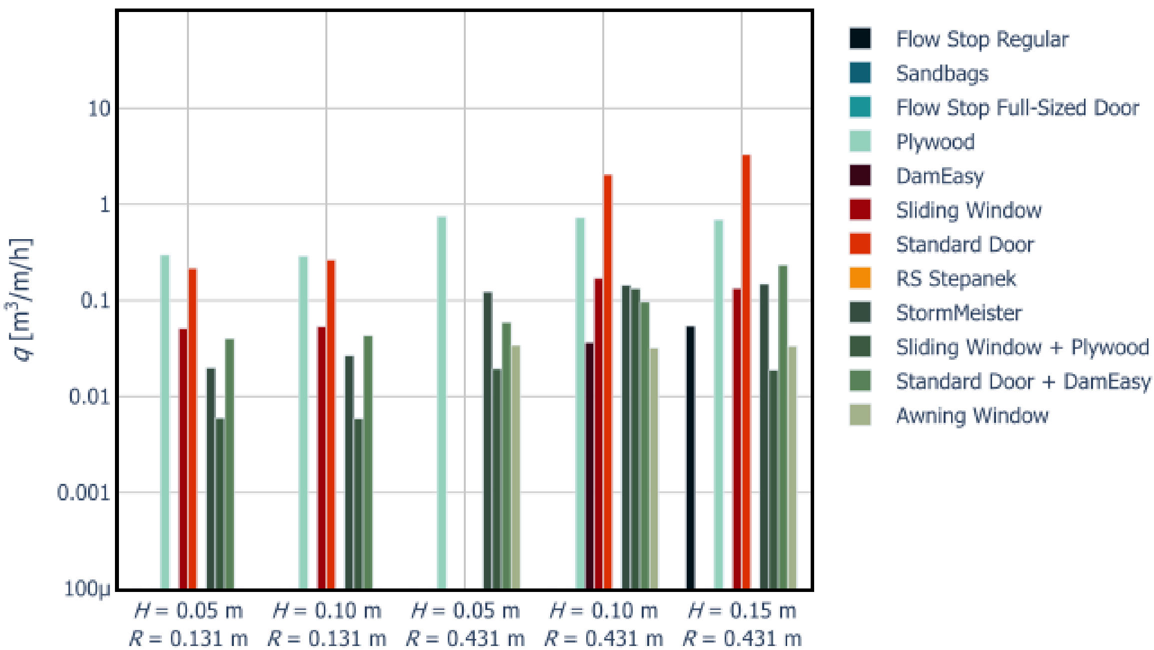

Figure 52. Average leakage rate per unit width for the wave experiments in Phase 2 (MWB only). The figure does not include tests from the IT as no waves were run in that facility.

5. Conclusions and Recommendations

This report presents the results of a comprehensive testing program that looked at the performance of standard Canadian construction of a residential home under flood loading (Phase 1) as well as the performance of several temporary opening barriers used on residential houses (Phase 2). The main conclusions of the report include:

- Water leakage through the residential home building envelope (not including any door or window openings) primarily occurred through the connection between the foundation and wooden structure.
- Leakage rates were primarily influenced by water depth (increasing water depths caused increasing leakage rates); wave conditions also influenced the leakage rate infiltrating the residential home.
- Temporary opening barrier performance was similarly influenced by water depth (increasing water depths caused increasing leakage rates).
- Opening barrier performance was also influenced by incident wave conditions, particularly in cases where overtopping the barrier could occur.
- Opening barrier leakage rates often differentiated the manufacturer’s estimated leakage rates, as well as the rates given for products that were previously tested to ANSI 2510 testing standards. This highlights the voracity of the testing data only to the unique installation conditions, and indicates the potential sensitivity of product performance to differences in installation.

This study assisted in the development of a comprehensive Canadian testing standard for temporary flood barriers using the National Research Council of Canada's Multidirectional Wave Basin in Ottawa, Ontario. The results of the testing showed notable differences from the ANSI 2510 protocol and the authors have the following recommendations for further research to build upon the study presented here:

- Repeat testing of various standard and historical Canadian building envelopes would help to further develop more accurate leakage rate estimations and expected ranges as a function of water depth. Repeat testing would also allow for a better understanding of the uncertainty of these estimations due to variances in building practices and quality of materials.
- Interdisciplinary research incorporating testing of the residential home wall damage and moisture content at the end of the test series would allow for an improved global understanding of building damage under flood loading. Also, long duration research into the relationship of flood exposure, and repeated flood exposure, to mold growth in Canadian home building products would also be of benefit.
- Development of clear guidance for the hydraulic testing facility and the construction and materials used for the flood barrier openings is needed to ensure consistent results between test protocols in different locations. This is needed to develop testing capabilities at multiple hydraulic laboratories, and develop trust in the relevance of any future testing standard.
- Increased transparency and communication on experimental testing protocols and test conditions for future standards to be better understand and be more relevant for the general public.
- Testing opening flood barriers to a future Canadian Standard should be completed and performed by untrained personnel only to the manufacturer's installation directions, and not installed by the manufacturer's trained installer (unless a certified installer is specifically required by the manufacturer in the installation directions).
- To test the durability of temporary flood barriers; several components are susceptible to damage with exposure to weather including sun exposure, freeze thaw, etc. A better understanding of the durability of these systems will inform their long-term use, storage, and any type of on-going maintenance.

6. Acknowledgements

The authors would like to acknowledge the funding provided by Architecture sans frontières Québec (ASFQ) and the Canadian Mortgage and Housing Corporation (CMHC) through the project "Référentiel des équipements résidentiels et des assemblages architecturaux pour faire face à l'inondation" of the Housing Supply Challenge: Round 4 - Building for the Future program. The authors would also like to acknowledge the essential help of the NRC Technical staff including: John Marquardt, Justin Hof-Macneil, Kyle Lambert and Maradona Laborde as well as the invaluable guidance provided by the Écohabitation team.

This project is being completed in collaboration with the NRC's Climate Resilient Built Environment Initiative, in support of delivering the Government of Canada's Adaptation Action Plan, and towards achieving commitments under the National Adaptation Strategy

7. References

ANSI. (2022). *American National Standard for Flood Mitigation Equipment ANSI/FM Approvals 2510-2022*.

Bernoulli, D. (1738). *Hydrodynamica*.

Biggar, K., & Masala, S. (1998). *Alternatives to sandbags for temporary flood protection*.

Biggar, K., & Srboljub Masala, Pe. (1998). *Alternatives to sandbags for temporary flood protection*.

Bramley, M., & Bowker, P. (2002). Improving local flood protection to property. *International Conference of Civil Engineering*.

British Standards Institution (2019). Flood Resistance Products: Perimeter barrier systems. Specification, pt. 2. *BSI Standards Publications,* BS 851188-2:2019.

CSA Group (2025). Temporary flood protection barriers hydraulic testing and performance Standard for Canadian climates. *Environment and Climate Change*. CSA W212 *(under public review - https://publicreview.csa.ca/Home/Details/5576)*.

Déom, C. (2024). *Synthèse des principaux enjeux, risques et pistes de solution pour adapter la conservation du patrimoine culturel bâti québécois aux impacts des changements climatiques.*

Déry, C., Barroca-Paccard, M., Thibault, M., Mailhot, A., & Stolle, J. (2023). La pensée design pour construire une séquence en éducation aux risques d'inondation: regard sur une collaboration intersectorielle. *ACFAS*.

Ellenrieder, T., & Rauch, E. (2024). *Flood risks on the rise*. Munich Re.

Environment and Climate Change Canada. (2024). *Government of Canada Adaptation Action Plan*.

Intergovernmental Panel on Climate Change (IPCC). (2023). *Climate Change 2022 – Impacts, Adaptation and Vulnerability*. Cambridge University Press. https://doi.org/10.1017/9781009325844

Krahn, T., Blatz, J. A., Alfaro, M., & Bathurst, R. J. (2007). Large-scale interface shear testing of sandbag dyke materials. *Geosynthetics International*, *14*(2), 119–126. https://doi.org/10.1680/gein.2007.14.2.119

Kreibich, H., Christenberger, S., & Schwarze, R. (2011). Economic motivation of households to undertake private precautionary measures against floods. *Natural Hazards and Earth System Science*, *11*(2), 309–321. https://doi.org/10.5194/nhess-11-309-2011

Lankenau, L., & Koppe, B. (2019). *Sandbagging versus Sandbag Replacement Systems: Costs, Time, Helpers, Logistics*. https://doi.org/10.5194/nhess-2019-165

Lankenau, L., Massolle, C., Koppe, B., & Krull, V. (2020). Sandbag replacement systems - A nonsensical and costly alternative to sandbagging? *Natural Hazards and Earth System Sciences*, *20*(1), 197–220. https://doi.org/10.5194/nhess-20-197-2020

Levasseur, É. (2021). *Cohabiter avec l'eau*.

Lohani, T. N., Matsushima, K., Aqil, U., Mohri, Y., & Tatsuoka, F. (2006). Evaluating the strength and deformation characteristics of a soil bag pile from full-scale laboratory tests. *Geosynthetics International*, *13*(6).

Massolle, C., Lankenau, L., & Koppe, B. (2018). Emergency flood control: Practice-oriented test series for the use of sandbag replacement systems. *Geosciences (Switzerland)*, *8*(12). https://doi.org/10.3390/geosciences8120482

McNeil, D. (2020). *An Independent Review of the 2019 Flood Events in Ontario*.

Molnia, B. F. (1973). Plastic Sandbags. *Science*, *181*(4104), 990–990. https://doi.org/10.1126/science.181.4104.990.b

NBC (2020). National Building Code of Canada 2020. Canadian Commission on Building and Fire Codes, National Research Council of Canada.

Ogunyoye, F., Stevens, R., & Underwood, S. (2011). *Temporary and demountable flood protection guide*. Environment Agency.

Pinkard, F., Pratt, T. C., Ward, D., Holmes, T., Kelley, J., Lee, L., Sills, G., Smith, E. W., Taylor, P., Torres, N., Wakeley, L., & Wibowo, J. (2007). *Flood-Fighting Structures Demonstration and Evaluation Program: Laboratory and Field Testing in Vicksburg, Mississippi*. https://www.researchgate.net/publication/235135012

Public Security Canada. (2022). *Adapting to Rising Flood Risk An Analysis of Insurance Solutions for Canada*.

Reeve, D., & Badr, A. (2003). Performance of sandbags for domestic flood defence. *Proceedings of the Institution of Civil Engineers*, 341–349.